OCS Study
BOEM 2023-033

Field Observations During Offshore Wind Structure Installation and Operation, Volume 2

U.S. Department of the Interior
Bureau of Ocean Energy Management
Office of Renewable Energy Programs

BOEM
Bureau of Ocean Energy Management

OCS Study
BOEM 2023-033

Field Observations During Offshore Wind Structure Installation and Operation, Volume 2

June 2023

Authors (in alphabetical order):
Kristen Ampela
Cathey E. Bacon
Anwar A. Khan
Ying-Tsong Lin
James H. Miller
Arthur E. Newhall
Gopu R. Potty

Prepared under BOEM Award
Contract No. M15PC00002
Task Order No. 140M0118F0006

By
HDR
369 Inverness Parkway, Suite 325
Englewood, CO 80112

U.S. Department of the Interior
Bureau of Ocean Energy Management
Office of Renewable Energy Programs

BOEM
Bureau of Ocean Energy Management

DISCLAIMER

Study concept, oversight, and funding were provided by the U.S. Department of the Interior, Bureau of Ocean Energy Management, Environmental Studies Program, Washington, D.C., under Contract Number M15PC00002, Task Order No. 140M0118F0006. This report has been technically reviewed by the Bureau of Ocean Energy Management, and it has been approved for publication. The views and conclusions contained in this document are those of the authors and should not be interpreted as representing the opinions or policies of the U.S. government, nor does mention of trade names or commercial products constitute endorsement or recommendation for use.

REPORT AVAILABILITY

To download a PDF file of this report, go to the U.S. Department of the Interior, Bureau of Ocean Energy Management website and search on 2023-033. The report is also available at the National Technical Reports Library at https://ntrl.ntis.gov/NTRL/.

CITATION

HDR. 2023. Field Observations During Offshore Wind Structure Installation and Operation, Volume 2. Final Report to U.S. Department of the Interior, Bureau of Ocean Energy Management, Office of Renewable Energy Programs. Contract No. M15PC00002. Report No. OCS Study BOEM 2023-033, pp 48.

ABOUT THE COVER

Cover photo: Coastal Virginia Offshore Wind Project Field Monitoring. Courtesy of HDR RODEO Team.

ACKNOWLEDGMENTS

1. The HDR Real-Time Opportunity for Development Environmental Observations (RODEO) Program Team includes the following subcontractors (in alphabetical order):

    - Arthur Popper, Ph.D.
    - Clark Group, LLC
    - EA Engineering Science & Technology, Inc.
    - Fugro Inc.
    - Fugro GB Marine Ltd.
    - H.T. Harvey & Associates
    - Loughine Limited
    - Subacoustech Environmental

2. Significant additional technical support for the RODEO Program monitoring reported in this volume was provided by the following institutions:

    - University of Rhode Island
    - Woods Hole Oceanographic Institution

3. The following Principal Investigators led and directed the monitoring and data analyses conducted for the Coastal Virginia Offshore Wind Projects:

    - Several Hydrophone Recording Units (SHRU) Vertical Line Arrays: Dr. Ying-Tsong Lin, Associate Scientist with Tenure, Applied Ocean Physics & Engineering Department, Woods Hole Oceanographic Institution
    - Geosled and Ocean Bottom Recorders Geophone and Hydrophone Sensor System (OBX): Professor James Miller, Chair, Department of Ocean Engineering and Dr. Gopu R. Potty, Research Professor, Department of Ocean Engineering, University of Rhode Island
    - Metocean and biofouling monitoring: Dr. Paul English, Fugro GB

Assistance and support from all team members was greatly appreciated.

Contents

List of Figures

List of Tables

List of Abbreviations and Acronyms

° or Deg	degrees
°C	degrees Celsius
BIWF	Block Island Wind Farm
BOEM	Bureau of Ocean Energy Management
CH	Channel
CTD	conductivity, temperature, and depth
CVOW	Coastal Virginia Offshore Wind Pilot Project
dB	decibel(s)
dB re 1 µPa	dB referenced to a pressure of 1 micropascal
DMME	Department of Mines, Minerals and Energy
DOI	Department of the Interior
Dominion	Dominion Energy, Inc
GB	gigabyte
Hz	hertz
kg/m^3	kilogram per cubic meter.
kHz	kilohertz
km	kilometer(s)
m	meter(s)
m/s	meter(s) per second
min	minute(s)
mm/s	millimeter(s) per second
MW	megawatt(s)
N	North
nm/s	nautical mile per second
NMFS	National Marine Fisheries Service
OBX	Ocean Bottom Recorders Geophone and Hydrophone Sensor System
Pa	pascal(s)
PAM	passive acoustic monitoring
PSU	Practical Salinity Unit
PTS	permanent threshold shift
µm/s	micrometers per second
$µm/s^2$	micrometers per second squared
µPa	micropascal
R/V	research vessel
RayDec	Random Decrement
rms	root mean square
RODEO	Real-Time Opportunity for Development Environmental Observations
rpm	revolutions per minute
Sec or S	second(s)
SHRU	Several Hydrophone Recording Units
SPL	sound pressure level
SSP	sound speed profile
TTS	temporary threshold shift
U.S.	United States
UTC	Coordinated Universal Time
V/µPa	volt per micropascal
W	West

Editorial Note

To facilitate presentation, review, and perusal of the large quantity of observations and data generated under Task Order 140M0118F0006, the task order deliverable was divided into the following three standalone volumes:

1. ***Volume 1***: contains methods, observations, data analyses, results, and conclusions from ***underwater acoustic monitoring*** conducted during the ***construction phase*** of the Maryland Meteorological Tower Project and the Coastal Virginia Offshore Wind Pilot Project.

2. ***Volume 2*** (this volume): contains methods, observations, data analyses, results, and conclusions from ***underwater acoustic monitoring*** conducted during the ***operational phase*** of the Coastal Virginia Offshore Wind Pilot Project.

3. ***Volume 3***: contains methods, observations, data analyses, results, and conclusions from ***turbidity, biofouling, and corrosion monitoring*** conducted during the ***operational phase*** of the Coastal Virginia Offshore Wind Pilot Project.

Executive Summary

This report presents methods, observations, data analyses, results, and conclusions from passive acoustic monitoring (PAM) surveys conducted during the ***operational*** phase of Coastal Virginia Offshore Wind Pilot Project (referred to as CVOW in this report). The monitoring was conducted under the United States (U.S.) Department of the Interior (DOI), Bureau of Ocean Energy Management's (BOEM) Real-Time Opportunity (RODEO) for Development Environmental Observations Program.

PAM data were recorded over approximately 40 days during the operational phase of CVOW to measure underwater sound levels within the water column and seafloor sediment vibrations generated by the revolving turbines. Data were collected using one Geosled; two Ocean Bottom Seismometers; and one RBRconcerto conductivity, temperature, and depth logger deployed approximately 1.3 kilometers from Turbine A01 and 352 meters (m) from Turbine A02.

Underwater noise levels recorded during turbine operations ranged from 120 to 130 decibels referenced to a pressure of 1 micropascal (dB re 1 µPa) except during storms, when the received levels increased to 145 dB re 1 µPa. Recorded particle acceleration levels were compared to published behavioral audiograms of selected fish species (e.g., Atlantic salmon [*Salmo salar*], dab [*Limanda limanda*], Atlantic cod [*Gadus morhua*], and plaice) and were found to be below the respective hearing thresholds for these species. Additionally, all recorded measurements at CVOW were below the temporary threshold shift (TTS) and permanent threshold shift (PTS) onset criteria for marine mammals recommended by the National Marine Fisheries Service[1].

Operational phase sound levels recorded at CVOW were higher (10 to 30 decibels [dB]) than those previously recorded at the Block Island Wind Farm (BIWF) at frequencies below approximately 120 hertz (Hz). It is hypothesized that the higher operational noise recorded at CVOW is due to vibrations in the monopile structures. The BIWF foundations are lattice-jacket structures with four legs and have no detectable structural vibrations. It is possible that the CVOW monopile foundations vibrate when the turbines are operating, and the vibrational energy is transmitted into the water column and seabed. This hypothesis needs additional investigation, both for the structural vibration mechanisms and potential biological effects.

At frequencies above 120 Hz, CVOW's operational phase monitoring results were broadly consistent with operational phase acoustic monitoring previously conducted at wind farms in the U.S. (BIWF) and Europe. At the BIWF, for example, underwater sound levels recorded at 50 m from operational turbines were near background (ambient) levels, and often not measurable due to other natural and anthropogenic noise (waves or boat sounds). Recorded sound levels at BIWF were also below the underwater TTS and PTS onset criteria for marine mammals. It should also be noted that lattice-jacket foundations were employed at BIWF, whereas monopile foundations were used at CVOW.

The data, results, conclusions, and recommendations presented in this report were generated for the U.S. DOI, BOEM, by the HDR RODEO Program Team under IDIQ Contract M15PC00002, Task Order 140M0118F0006.

[1] the behavioral harassment threshold for non-impulsive sound is 120 dB, and the TTS and PTS thresholds mentioned are above 150 dB (metric is the weighted cumulative sound exposure level).

1 Introduction

This report presents methods, observations, data analyses, results, and conclusions from passive acoustic monitoring (PAM) surveys conducted under the United States (U.S.) Department of the Interior Bureau of Ocean Energy Management's (BOEM) Real-Time Opportunity for Development Environmental Observations (RODEO) Program. The monitoring was conducted during the ***operational*** phase of the Coastal Virginia Offshore Wind Pilot Project[2] (referred to as CVOW in this report). PAM was conducted within the project area under the RODEO Program. Lessons learned from monitoring conducted under the RODEO Program will guide future commercial wind energy development in the U.S.

1.1 RODEO Program

The purpose of the RODEO Program is to make direct, real-time measurements of the nature, intensity, and duration of potential stressors during the construction and initial operations of selected proposed offshore wind facilities. The purpose also includes recording direct observations during the testing of different equipment types that may be used during future offshore development to measure or monitor activities and their impact-producing factors (stressors).

BOEM conducts environmental reviews, including National Environmental Policy Act analyses and compliance documents, for each major stage of energy development planning, including leasing, site assessment, construction, operations, and decommissioning. These analyses include 1) identification of impact-producing factors and receptors such as marine mammals and seafloor (benthic) habitats; and 2) evaluation of potential environmental impacts from the proposed offshore wind development activities on human, coastal, and marine environments. The analyses require estimations of impact-producing factors such as noise and the effects of the stressor on the ecosystem or receptors. Describing the impact-producing factors requires knowledge or estimates of the duration, nature, and extent of the impact-generating activity.

BOEM may use the RODEO Program monitoring data as inputs to analyses or models that evaluate the effects of future offshore wind turbine construction and operations, as well as facilitate operational planning that would reduce potential impacts to the greatest extent possible. The understanding and insights gained from the RODEO Program data analyses will help BOEM identify, reduce, and mitigate environmental risks in the future, and significantly increase the efficiency and efficacy of BOEM's regulatory review process for offshore wind development in the U.S. Finally, RODEO Program data will support the prioritization of future monitoring efforts and risk retirement. For example, if the RODEO Program monitoring data indicates the likelihood of impacts from a particular project development phase is low or inconsequential, then such phases may not be monitored during future projects.

It is important to note that the RODEO Program is not intended to duplicate or substitute for any monitoring that the developers of the proposed projects may otherwise require to be conducted. Therefore, RODEO Program monitoring is limited to selected parameters only. Also, RODEO Program monitoring is coordinated with the industry and is not intended to interfere with or result in a delay of industry activities.

[2] Methods, observations, data analyses, results, and conclusions from environmental monitoring surveys conducted during the ***construction*** phase of CVOW were previously reported in Volume 1 (HDR 2020).

All RODEO Program field activities were conducted in accordance with a BOEM-approved Field Sampling Plan, which included a project-specific Health and Safety Plan[3].

1.2 Coastal Virginia Offshore Wind Pilot Project

Dominion Energy, Inc. (Dominion) operates CVOW, which is located 27 miles off the coast of Virginia Beach, Virginia, on an 8.6-square-kilometer (2,135-acre) site leased by the Virginia Department of Mines, Minerals, and Energy (DMME). This is the first offshore wind farm within federal waters and the second to become operational within the U.S.

Dominion had an agreement with the Virginia Department of Energy (formerly known as the DMME) to build and operate two 6-megawatt (MW) wind turbines on monopile foundations at this site during the first (pilot) phase of the project. The turbine location (**Figure 1**) coordinates are:

- Turbine A01: Latitude 36 degrees (°) 53.7772 North (N); Longitude 75° 29.4980 West (W)
- Turbine A02: Latitude 36° 53.2100 N; Longitude 75° 29.4943 W

During the pilot phase of this project, two monopile turbine foundations were installed by pile driving on 25 and 30 May 2020. Each monopile has a 7.8-meter (m) diameter and an approximately 67-m length. A 34-kilovolt submarine power distribution line that runs from the turbines to a connection point in Dominion's electrical system near Camp Pendleton was subsequently installed. The transmission line is buried approximately 2 m under the seabed for much of its length, and it comes ashore through a 1,000-m conduit installed under the beach.

Initial operations and testing of the turbines were completed in October 2020. The two turbines generate 12 MW of energy.

1.3 Report Organization

Key results, observations, and conclusions from environmental monitoring conducted during the construction of offshore wind structures at the two sites are summarized in individual sections of this report. Selected raw data and detailed discussions are contained in technical reports, which are provided as digital appendices to this summary report. This report is organized as follows:

- **Section 1** presents an overview of the RODEO Program and includes a summary description of CVOW.
- **Section 2** contains methods, results, and conclusions from CVOW's operational phase of PAM.
- **Section 3** lists the references cited in this report.
- **Appendix A** includes the hydrophone and geophone sensitivity curves.

[3] See Volume 1 (HDR 2020) for a copy of the Field Sampling Plan and Health and Safety Plan.

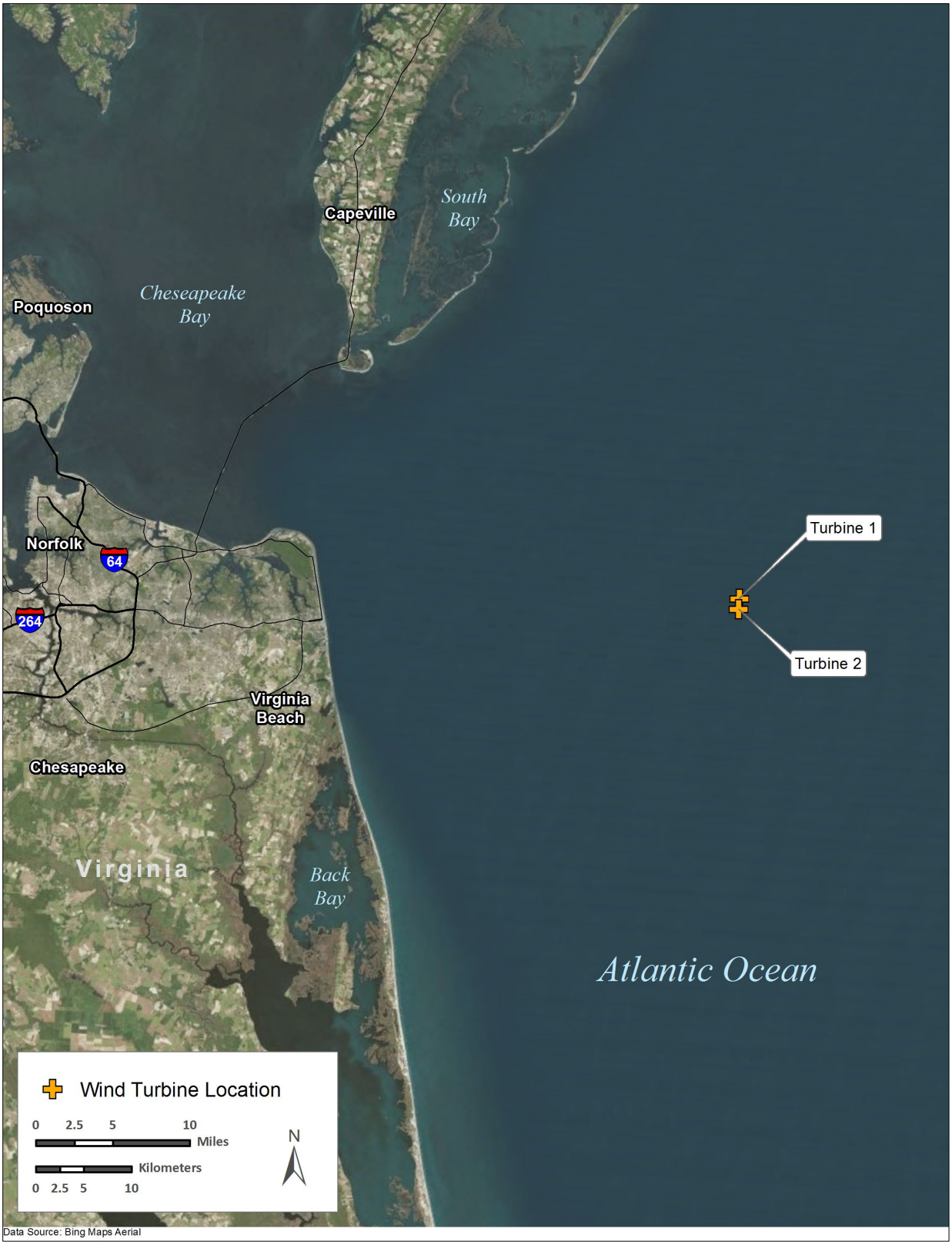

Figure 1. Location of the two CVOW Pilot Project monopile turbines

2 CVOW Operational Phase Passive Acoustic Monitoring

Noise from operational turbines is caused by the rotation of the wind-powered components, which generate mechanical vibrations in the nacelle that are transmitted down to the turbine foundation and into the surrounding water column and seabed. The correlation of mechanical vibrations of the turbine tower with sound pressure and particle motion measurements within the water column has been reported by several studies, including Lindell (2003) and Sigray and Andersson (2011), and is supported by model simulations (Marmo et al. 2013).

Under BOEM's RODEO Program, PAM data were recorded over approximately 40 days during the operational phase of CVOW to measure and analyze underwater sound levels within the water column and seafloor sediment vibrations generated by the revolving turbines.

2.1 Monitoring Objectives

PAM was conducted to measure and analyze underwater sound levels within the water column and seafloor sediment vibrations generated by the operating turbines. Data were collected over an approximately 40-day period from 13 December 2021 to 24 January 2022.

2.2 Methods and Data Recording Systems

Data were collected using one Geosled; two Ocean Bottom Seismometers; and one RBRconcerto conductivity, temperature, and depth (CTD) logger deployed approximately 1.3 kilometers (km) from Turbine A01 and 352 m from Turbine A02. Additional details on the data recording systems are presented below:

1. Geosled
    a. Two Several Hydrophone Recording Units (SHRU) data acquisition systems (four channels each) housed in a Geosled
    b. One tetrahedral hydrophone array and one geophone (three-axis particle velocity and a hydrophone). The spacing of the hydrophones in the tetrahedral array was 52 centimeters.
    c. Seascan clocks
    d. Geo SHRU: 256 gigabytes (GB), approximately 10-kilohertz (kHz) sampling rate with pseudo-24-bit data
    e. Three-axis geophone with a co-located hydrophone connected to the geo SHRU
    f. Tetrahedral SHRU: 256 GB, approximately 20-kHz sampling rate with true 24-bit data
    g. Fixed 26-decibel (dB) gain on all SHRUs
    h. High-sensitivity (-170 dB referenced to 1 volt per micropascal [V/µPa]) hydrophones on tetrahedral
2. Two ocean bottom seismometers (Ocean Bottom Recorders Geophone and Hydrophone Sensor Systems [OBX] 14396 and 4010)
    a. Sampling rate of 2 kHz for 50 days, limited by batteries
    b. 128 GB, true 24-bit data on all channels
    c. Pre-amp gains set to 24 dB on all channels
    d. Chip-scale atomic clocks
3. One RBRconcerto CTD logger
    a. One on Geosled
    b. 30-second sampling rate

All stationary moorings were deployed on 14 December 2021 at 13:00 Coordinated Universal Time (UTC) using the research vessel (R/V) *Virginia*; the scientific party included scientists and engineers from

the University of Rhode Island and Woods Hole Oceanographic Institution. The moorings were recovered using the same vessel on 2 February 2022 at 19:00 UTC. The batteries powering the recording units lost power on 22 to 24 January 2021, at which point data collection stopped.

Sound speed profiles (SSPs) were measured using a CTD device during both deployment and recovery cruises. Specifically, a CTD logger was attached to the Geosled to 1) obtain a water column CTD and SSP during the sled deployment, 2) monitor the environment over the entire deployment cycle, and 3) obtain a water column profile at the sled recovery. Wind and turbine rotational speed data for the duration of deployment were obtained from the project owners and used for data analysis.

The Geosled and two OBX moorings were deployed approximately 1.3 km from Turbine A01 and 352 m from Turbine A02 (**Table 1**, **Figure 2**). All sensors were deployed to the east of the turbines to avoid contact with the submarine cable. **Figure 3** shows the data coverage of the Geosled geophone (top panel) and tetrahedral hydrophone (bottom panel).

Figure 4 shows the Geosled mooring showing the nominal positions of the three-axis geophones and two OBXs. The orientation of the OBXs were available through the heading sensor. Based on the heading sensor readings, the OBX 14010 and 14396 were oriented such that the angle between the propagation path and the inline axis were 18 degrees and 32 degrees (northern turbine), respectively. These angles were 3 degrees and 11 degrees for the southern turbine, respectively. **Figure 5** shows the OBX with the inline, cross line, and vertical axes. **Appendix A** presents hydrophone and geophone sensitivity curves.

Table 1. PAM data recording systems deployed at CVOW

Systems	Data Collection Objective	Sampling Rate (kHz)	Location	Distance from Turbine A01 (km)	Distance from Turbine A02 (m)	Water Column Depth (m)	Comments
Geosled with Tetrahedral Hydrophone Array and a Three-Axis Geophone	Short-range particle velocity within the water column and at the seabed; pressure signal at a fixed range	10	36° 53.062 N 75° 29.345 W	1.3	352	26	The SHRU data disks filled up and stopped sampling on 21 January 2022 (for the tetrahedral array hydrophones) and 24 January 2022 (for the three-axis geophone)
OBX Geophone and Hydrophone Sensor System	Range dependence of short-range particle velocity within the water column and at the seabed; pressure signal	2	36° 53.062 N 75° 29.345 W	1.3	352	26	The OBXs stopped recording on 21 January 2022 (since they had been switched on the day before, they were shipped to the site during the last week of November 2021)

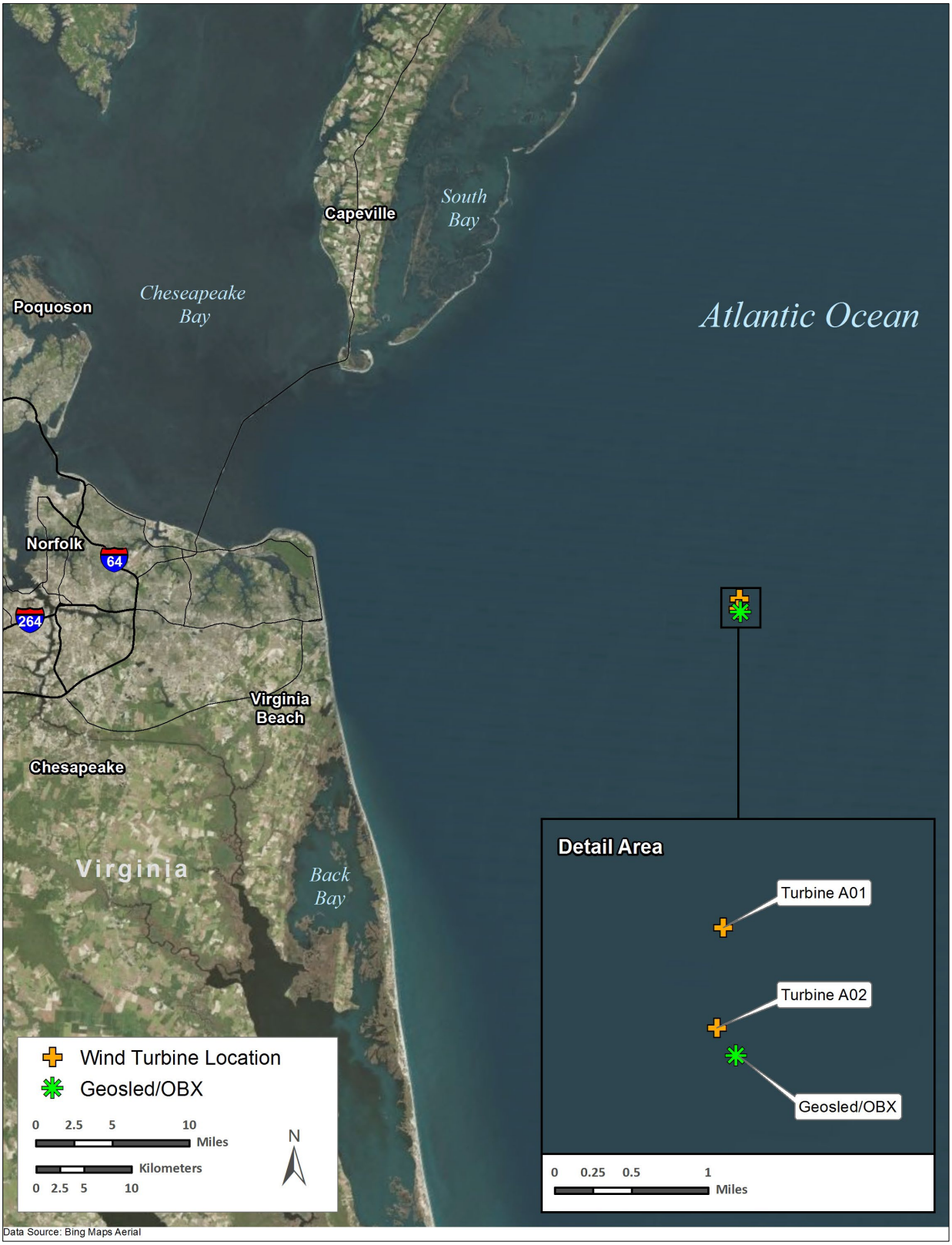

Figure 2. Geosled and OBX mooring locations

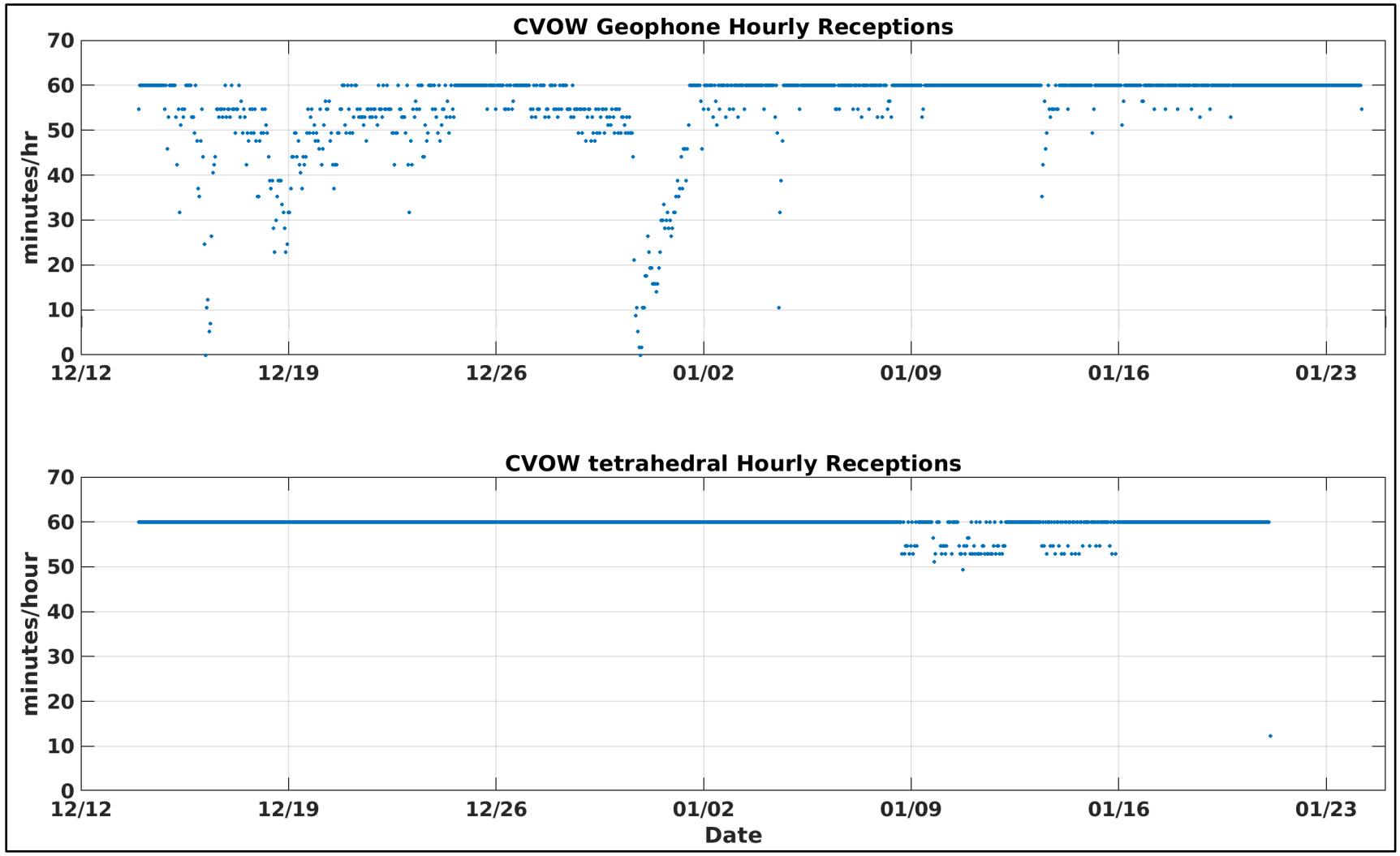

Figure 3. Data coverage of the Geosled geophone (top) and tetrahedral hydrophone (bottom)

Note: Y-axis shows the successful receptions in minutes per every hour of deployment. The geophone SHRU had more dropouts compared to the tetrahedral hydrophone SHRU.

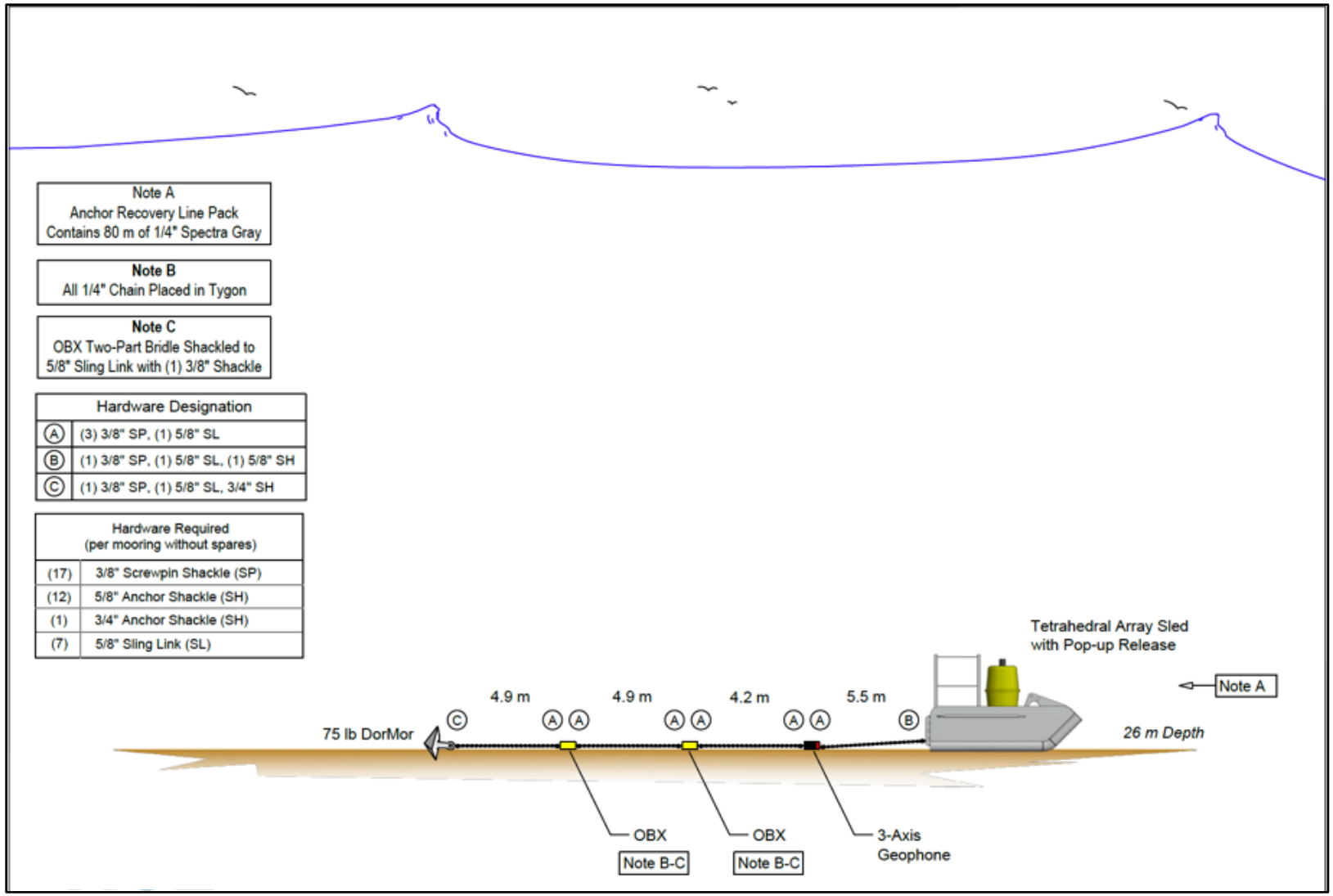

Figure 4. Mooring diagram for the Geosled, showing the sensor spacings

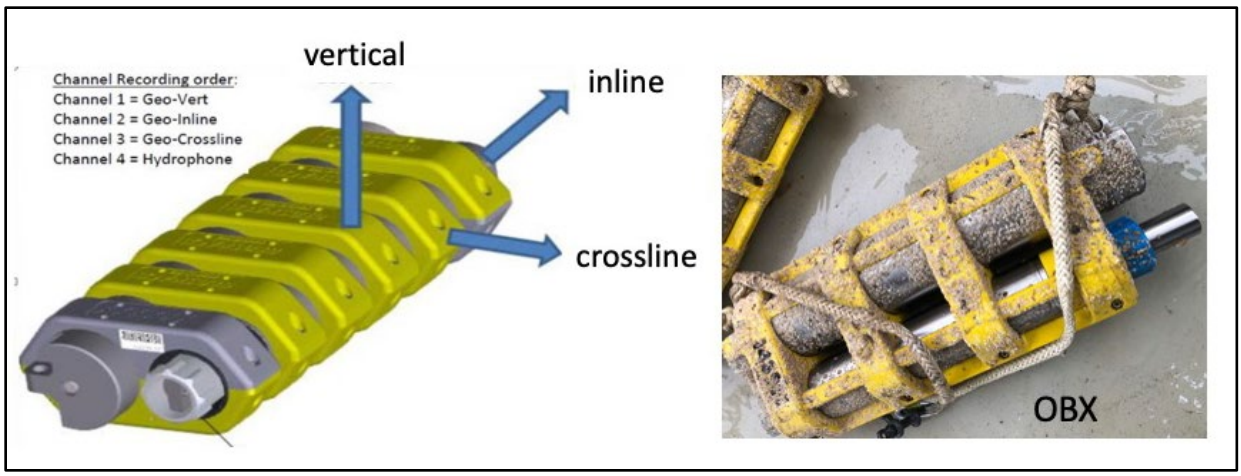

Figure 5. OBX with the inline, cross line, and vertical axes defined (left); OBX after recovery on the deck of the research vessel (right)

2.3 Data Analyses and Key Results

Key results from analyses of data collected using the 1) RBRconcerto CTD logger (associated with the Geosled), 2) OBX, and 3) tetrahedral array are presented in **Subsections 2.3.1**, **2.3.2**, and **2.3.3**, respectively.

2.3.1 RBRconcerto CTD Logger Data Analysis

Figures 6 and **7** show temperature, salinity, sound speeds, and pressure (depth) data recorded by the RBRconcerto CTD logger mounted on the Geosled. Data indicated a reduction in water temperature of approximately 5 degrees Celsius (°C) over the deployment period. In-water sound speeds decreased by approximately 20 meters per second (m/s) over the same period. The average water depth recorded was 26.25 m, with a tidal range of more than 1 m (**Figure 7**).

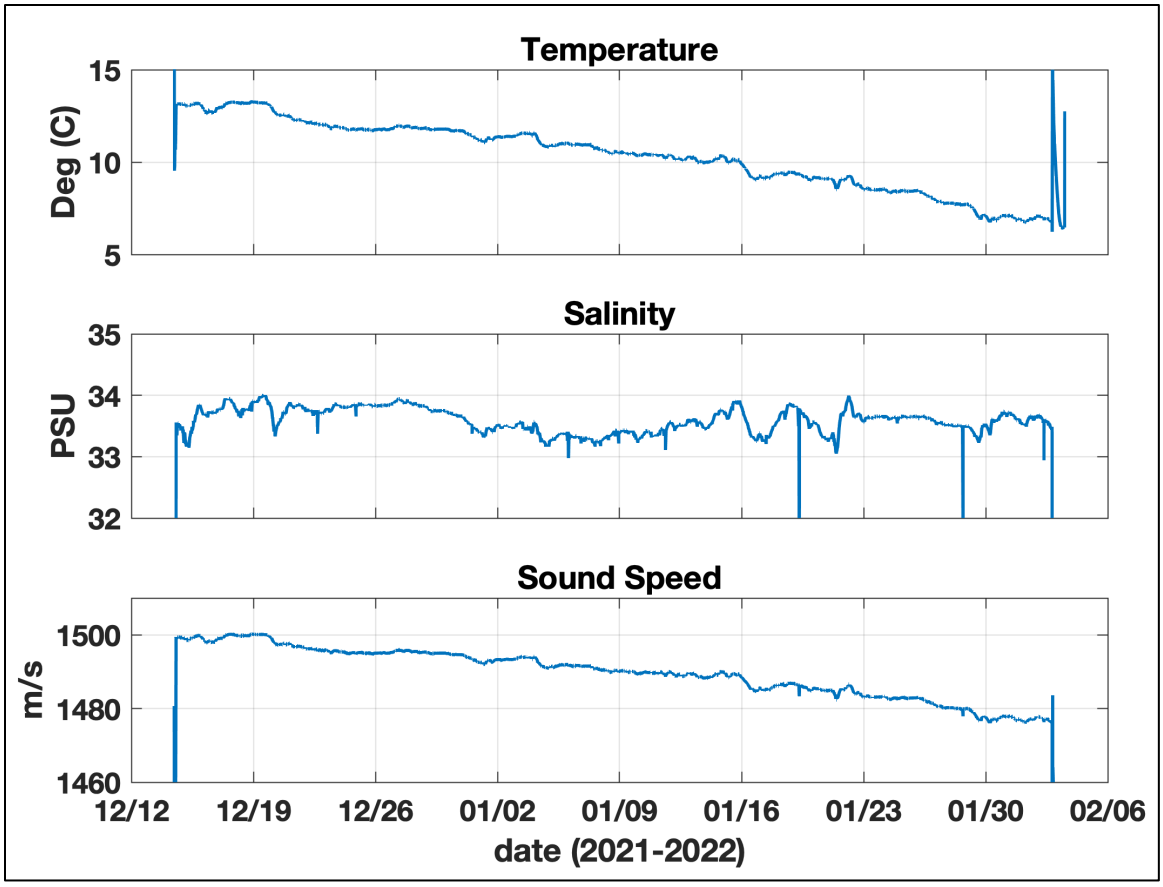

Figure 6. Temperature, salinity, and sound speed data

Note: Deg = Degree; PSU = Practical Salinity Unit

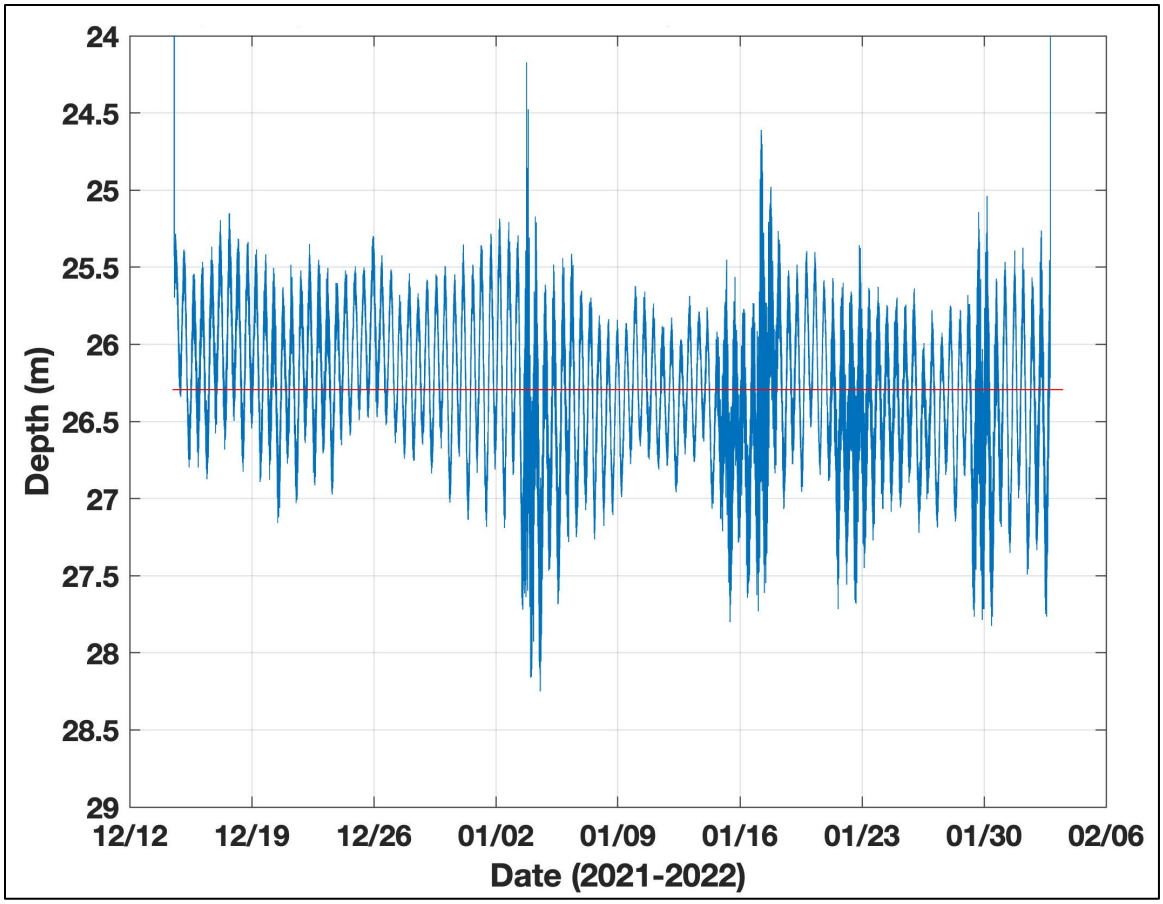

Figure 7. Mean water depth and the tidal variation data

The left and right panels of **Figure 8** show the temperature, salinity, and SSPs as a function of depth measured during deployment and recovery, respectively. The February profile (right panel) is iso-velocity in nature, and the December profile (left panel) shows surface cooling.

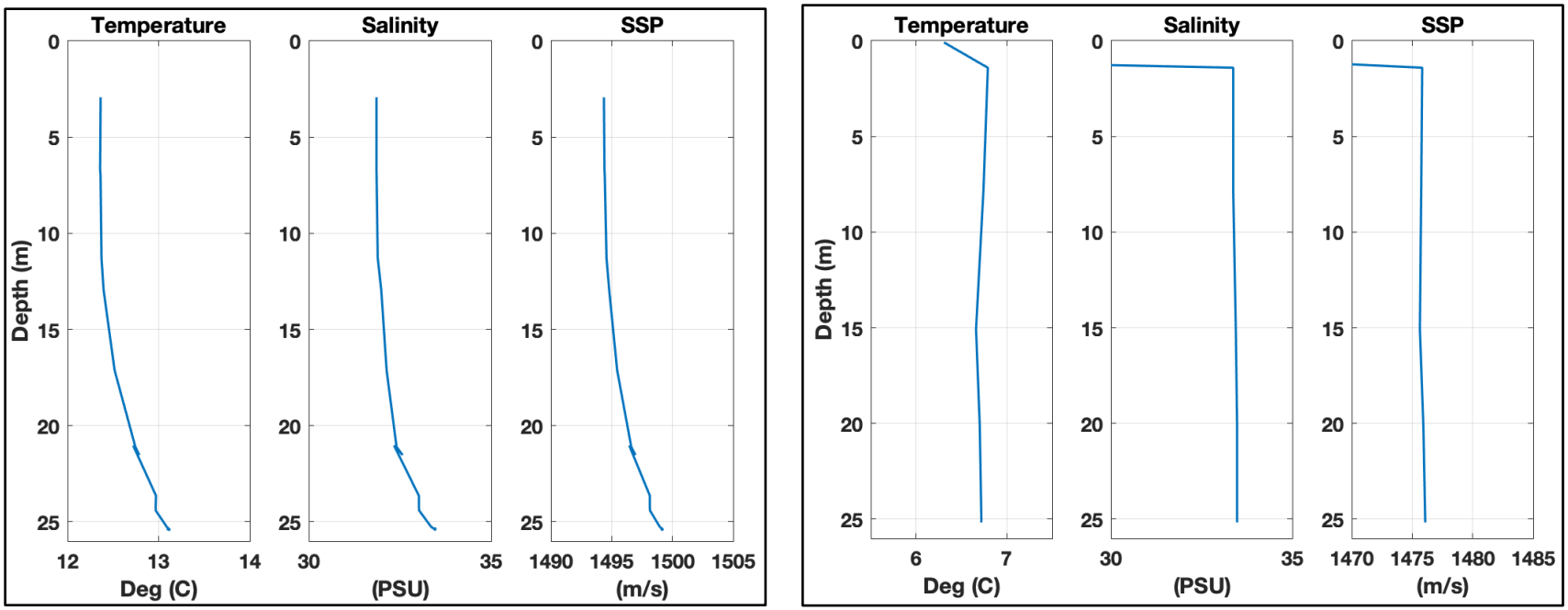

Figure 8. Temperature, salinity, and SSPs measured during the 14 December 2021 deployment at 13:00 UTC (left panel) and 2 February 2022 recovery at 19:00 UTC (right panel)

Notes: Deg = Degree; PSU = Practical Salinity Unit

2.3.2 OBX Data Analysis

In addition to compressional wave (P-wave) and shear wave (S-wave), the sea bottom, depending on the rigidity of the sediments, may support other types of waves. An example are interface waves, which travel along the boundaries of two media. For an interface between water and sediment, two types of interface waves are possible: Love waves and Scholte waves. Scholte waves result from a combination of P and SV (vertically polarized shear wave) motions, while Love waves result from SH (horizontally polarized shear waves trapped near the interface). The energy carried by interface waves decays with distance r from the source as 1/r. These waves are slightly slower than the shear waves, and they arrive at a receiver after the P- and S-waves arrive. Scholte waves have maximum amplitude at the interface, and the amplitude reduces exponentially with distance away from the interface on both media.

Increasing evidence suggests that anthropogenic substrate-borne energy is likely to adversely affect benthic invertebrates (Roberts and Elliot 2017). The results of experiments conducted by Roberts and Elliot (2017) indicate that animals are sensitive to, and respond directly to, anthropogenic stimuli propagating within the sediment. The Roberts and Elliot (2017) study concluded that in the aquatic environment, management and consenting procedures concerning anthropogenic sources should not only consider water-borne acoustic energy but should also include the potential impact of sediment vibration. Measurement of seabed vibration in our study using OBX is an important step toward understanding the impact on benthic invertebrates.

Figure 9 shows the root mean square (rms) values calculated from the OBX data for the deployment duration. The rms values are calculated over 1-minute time windows for the three particle velocity components (vertical, inline, and cross line) and acoustic pressure (hydrophone data) starting on 15 December 2021 at 00:00:00 UTC. The left panel in **Figure 9** corresponds to OBX 14010, and the right panel corresponds to OBX 14396. The rms particle velocity and pressure values measured on the two OBXs seem to be very similar on both OBXs, and some of the peaks correspond to increased wind/wave activity.

Figure 10 shows an example time series of particle velocity components (in millimeters per second [mm/s]) and acoustic pressure (in pascals [Pa]) of 10-minute duration (left panel). The data corresponds to 12 January 2022, starting at 08:02:00 UTC. The waves during this time were approximately 0.7 to 0.75 m (significant wave height), and the wind speed was 5 to 6 m/s. The two turbines were rotating at 9 to 10 revolutions per minute (rpm) during this period. The range of values for the particle velocity amplitudes (u) and pressure (p) (y-axis range) is related through the characteristic impedance of water (ρc) (assuming plane propagating waves) as follows:

$$p = \rho c \boldsymbol{u}$$

Based on the plane wave assumption, assuming sound speed and density of 1,500 m/s and 1,000 kilograms per cubic meter (kg/m^3), for an acoustic pressure magnitude of 5 Pa, the particle velocity should be equal to 3.3 micrometers per second (μm/s). It should be noted that this is an approximation since the plane wave assumption is not entirely correct. This check is only meant to be an order of magnitude comparison.

Therefore, the range of particle velocity values seems reasonable. The right panel in **Figure 10** shows the spectrogram of a portion of the data, of 1 minute duration, shown on the left panel. Tonals can be seen in all channels.

The tonals present in the particle velocity and pressure data can be clearly seen in the power spectral density diagrams (**Figure 11**). The left panel in **Figure 11** shows the power spectral density calculated using Welch's periodogram methods for the three-particle velocity components, and the right panel shows

the same for acoustic pressure. The low frequencies appear to contain considerable energy, both in the pressure and particle velocity components.

Figure 12 is similar to **Figure 10** and shows the time series (left panel) and spectrogram (right panel). The data correspond to a different day (3 January 2022; 17:19:00 UTC). The left panel (time series) is plotted for a duration of 10 minutes and the spectrogram (right panel) is for a duration of 1 minute. Note that the range of pressure and particle velocity amplitudes are much higher for this day (approximately 20 times). This period corresponds to very strong wave activity, with significant wave heights reaching approximately 4 m.

The right panel of **Figure 13** shows the sound pressure level (SPL) in dB referenced to 1 micropascal (dB re 1 μPa). The data from two OBXs (shown in red and black) overlap as they were separated by only 5 m. The left panel in **Figure 13** is published data from Tougaard et al. (2020), showing the SPL as a function of turbine size. Note that, in this figure, the measurements have been normalized to a distance of 100 m and a wind speed of 10 m/s. Solid lines represent best fitting straight lines, and broken lines indicate the standard error. Based on the trend line and the standard errors, for a 6 MW turbine, the SPLs will be approximately in the range 110 to 125 dB re 1 μPa. CVOW measurements seem to be within the range of values shown in the historical data. Note that this is only a very approximate comparison as the effect of many other parameters (e.g., wind speed, range, environmental and bottom conditions) needs to be considered to make an apt comparison.

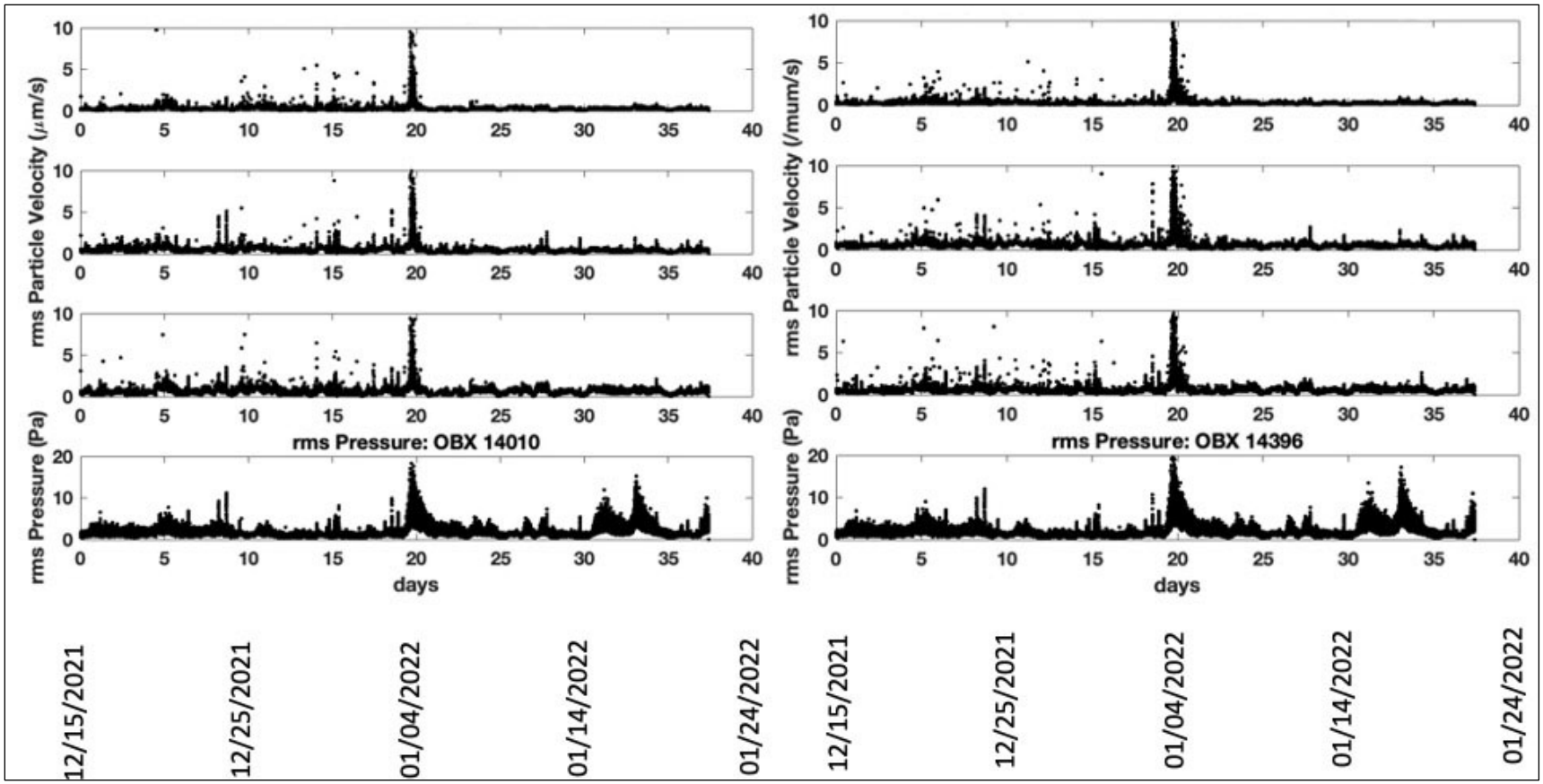

Figure 9. Rms values calculated from the OBX data (OBX 14010 [left panel] and OBX 14396 [right panel]); the four panels (from top to bottom) are the vertical, inline, and cross line particle velocity components and acoustic pressure, respectively.

Note: The rms values are calculated over 1-minute time windows for the three particle velocity components (vertical, inline, and cross line) and acoustic pressure.

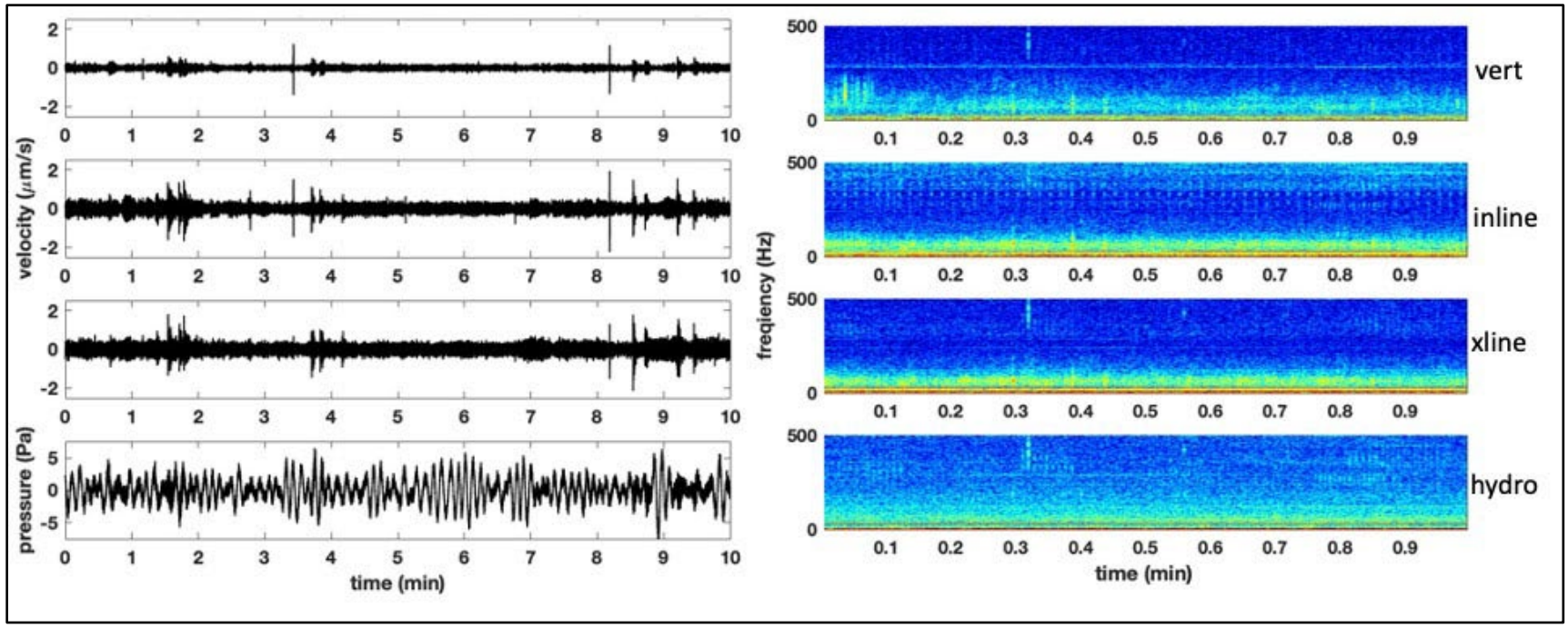

Figure 10. Particle velocity (top three subplots) and acoustic pressure (bottom subplot) measured on OBX 14396 on 12 January 2022, starting at 08:02:00 UTC (left panel)

Note: The right panel shows the spectrogram of the signals shown on the left.
μm/s = micrometers per second; min = minute(s); vert = vertical; xline = cross line

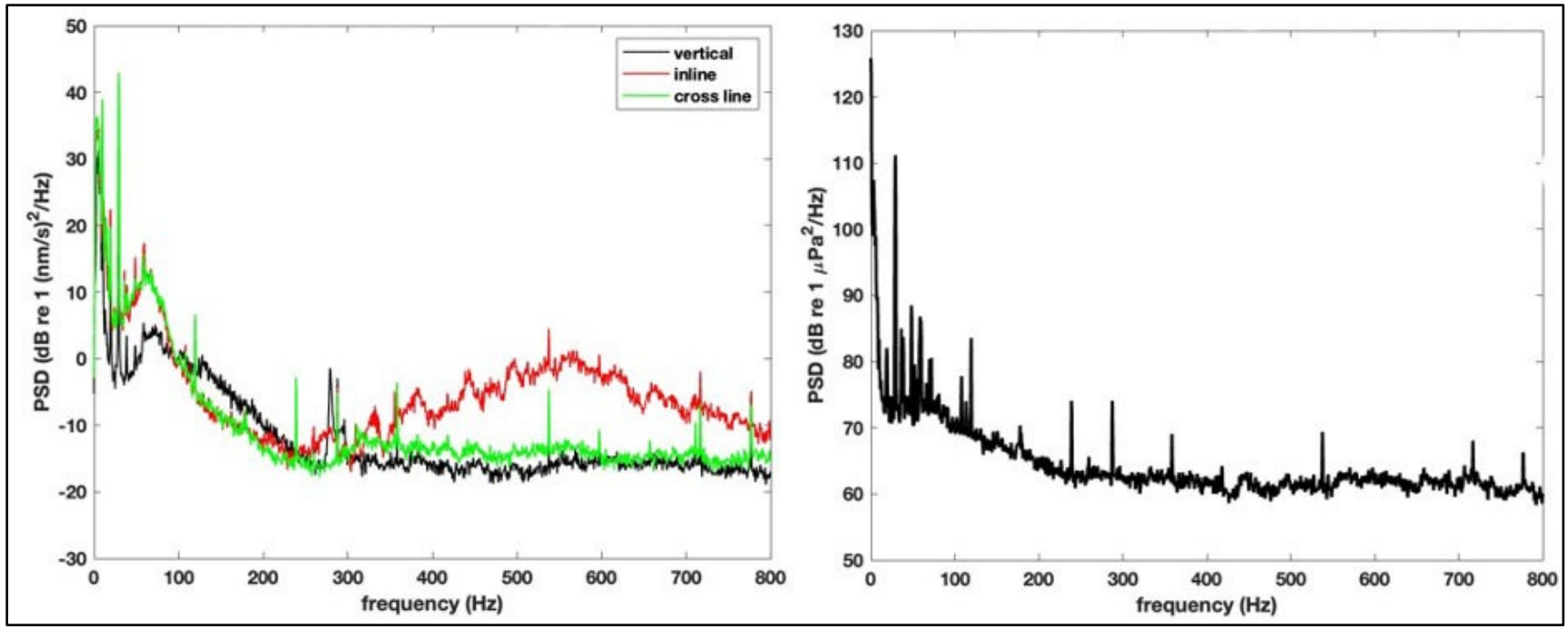

Figure 11. Power spectral density calculated using Welch's periodogram methods for the three-particle velocity components (left panel), with the same for acoustic pressure (right panel)

Note: The data correspond to 12 January 2022, 08:02:00 UTC.
Hz = hertz; nm/s = nautical mile per second

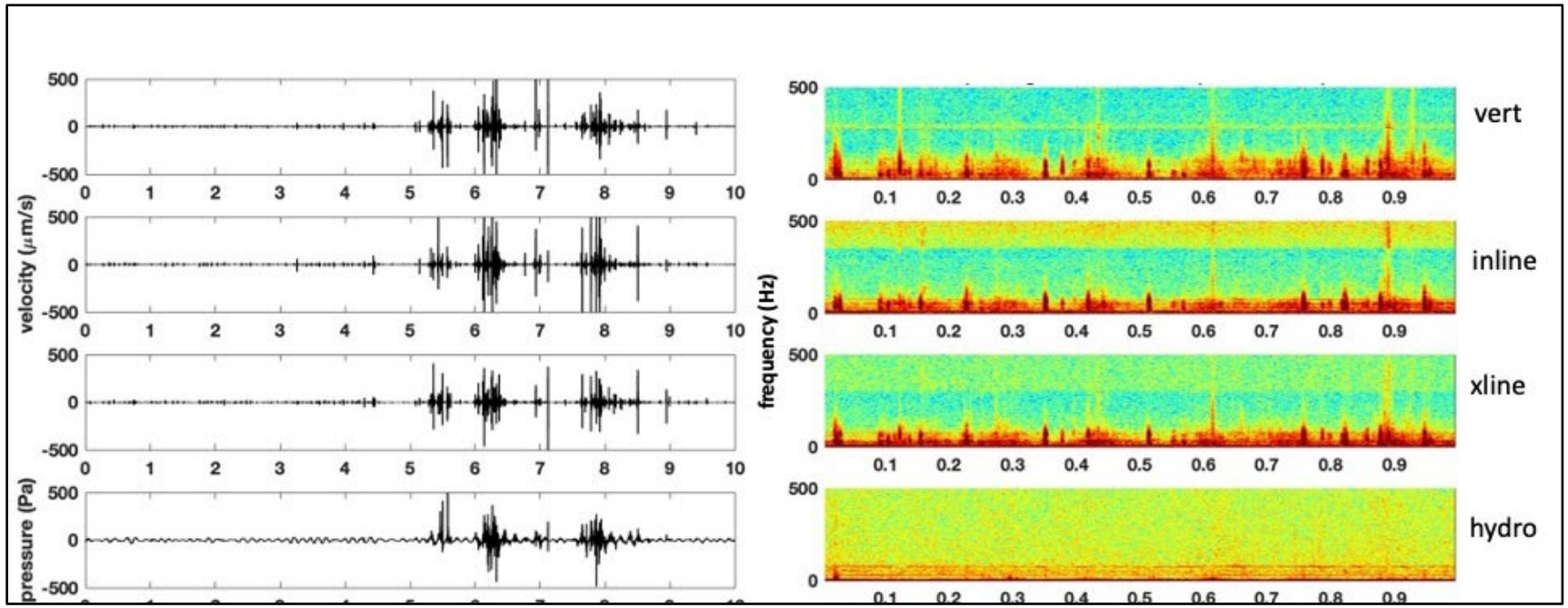

Figure 12. Three-particle velocity components and the acoustic pressure measured on the OBX (left panel) from 3 January 2022 at 17:09 UTC

Note: The right panel shows the spectrogram of the acoustic pressure and particle velocity. The x- axis on the right panel shows a total duration of 1 minute, while the left panel shows a total duration of 10 minutes. Data correspond to 3 January 2022, 17:19:00 UTC.
Hz = hertz; μm/s = micrometers per second; min = minutes; vert = vertical; xline = cross line

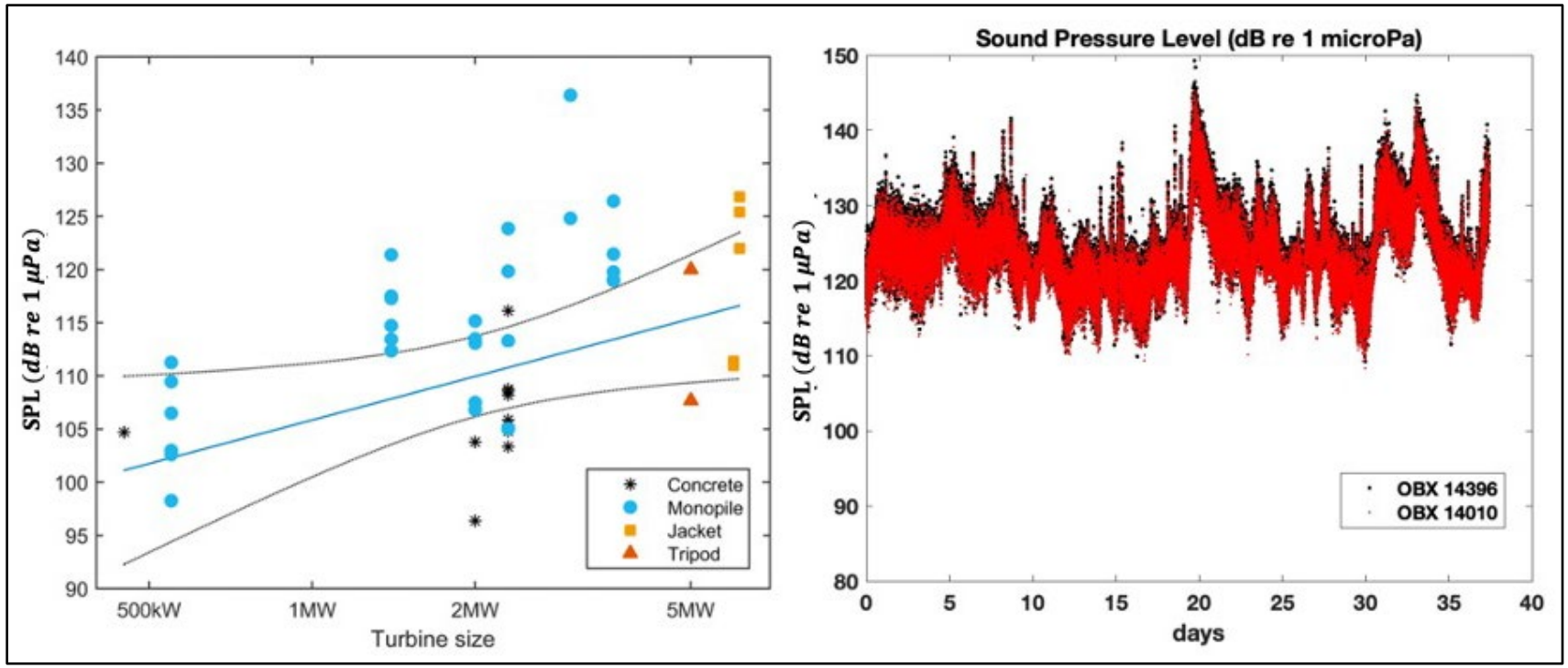

Figure 13. SPLs produced by wind turbines of different sizes measured at 100 m and at a wind speed of 10 m/s

Source: Tougaard et al. 2020
Note: Solid lines represent best fitting straight lines, and broken lines indicate the standard error. The right panel shows the data from the two OBXs.

To understand the impact of interface (Scholte) waves, a technique used extensively in geophysical community called Random Decrement (RayDec) was applied to the data collected by the OBX. RayDec is a fast and simple method to identify interface waves and determine the azimuth of these arrivals. It suppresses Love and other body waves efficiently. The azimuth angles are searched for in such a way that it maximizes the correlation between vertical and horizontal particle motion components of the Scholte waves. The correlation is performed after shifting the horizontal components by a quarter period to compensate for the natural phase shift between vertical and horizontal components of interface waves (Hobiger et al. 2009).

Figure 14 (left panel) shows the direction of arrival of Scholte waves estimated using the RayDec technique. Arrivals having high correlation between the vertical and horizontal particle motion components of the Scholte waves only are shown in this figure. **Figure 14** shows significant Scholte wave arrivals in the low frequencies (less than 40 hertz [Hz]). They seem to come from approximately 300° azimuths. The exact direction can be calculated based on the orientation of the OBX, which will provide information about the potential source of the Scholte wave energy. **Figure 14** (right panel) shows the acoustic pressure spectral density after filtering out the Scholte wave arrivals. The tonals can be very clearly seen. The data correspond to 12 January 2022 (shown in **Figure 11**).

The particle acceleration was also calculated from the measured particle velocity, and **Figure 15** shows an example (data corresponds to 12 January 2022 at 08:02:00 UTC). The particle acceleration is expressed in dB referenced to 1 micrometer per second squared ($\mu m/s^2$) so it can be compared to published behavioral audiograms of fish (e.g., Atlantic salmon [*Salmo salar*], dab [*Limanda limanda*], Atlantic cod [*Gadus morhua*], plaice). These hearing sensitivity curves can be compared to the particle acceleration levels for the vertical, inline, and cross line components.

It can be seen that the particle acceleration levels are below the hearing threshold of all fish considered here. This result is similar to what was observed near the operating wind turbines in the Block Island Wind Farm (BIWF) (HDR 2019). **Figure 15** (right panel) shows the result from the BIWF (note that only the vertical particle acceleration component is shown for the BIWF). It should also be noted that lattice-jacket foundations were employed at BIWF, whereas monopile foundations were used at CVOW.

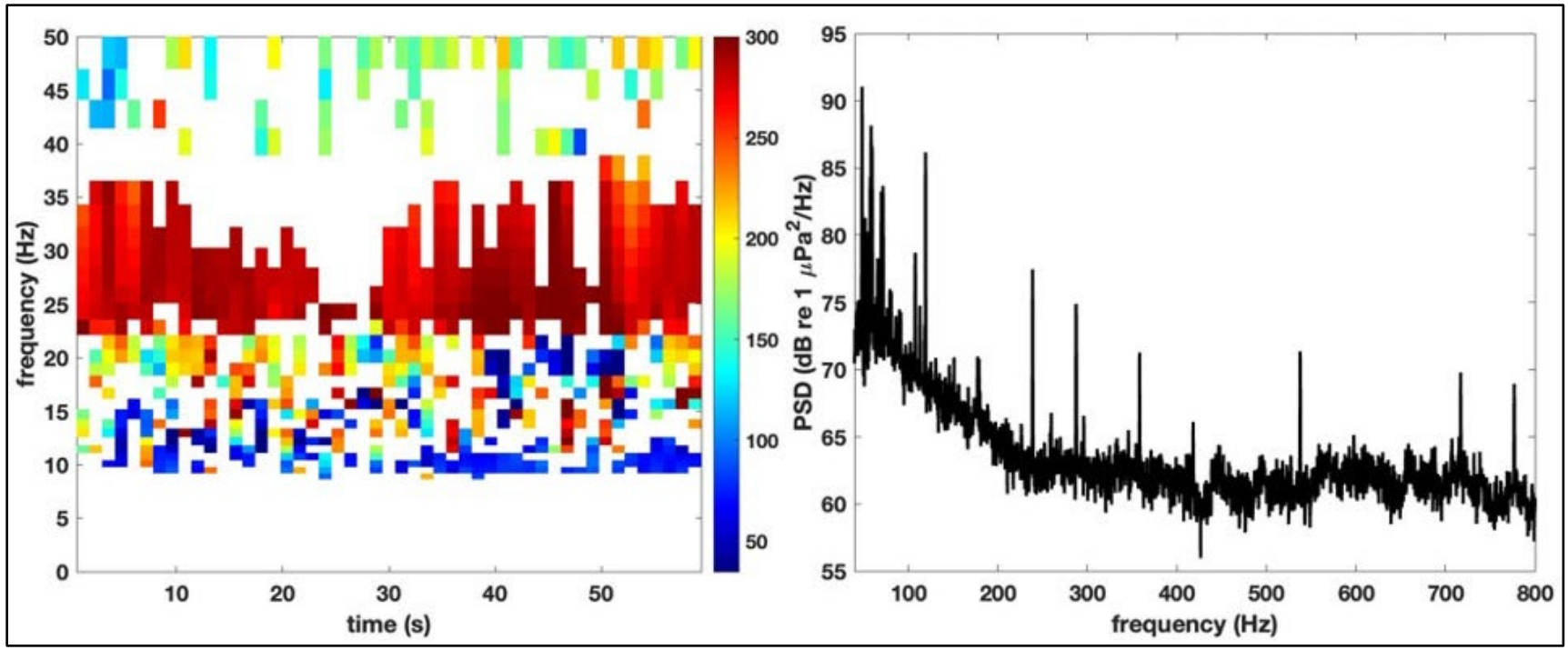

Figure 14. Direction of arrival of Scholte waves (left panel) estimated using the RayDec technique

Note: The right panel shows the acoustic pressure spectral density after filtering out the Scholte wave arrivals.
s = second(s)

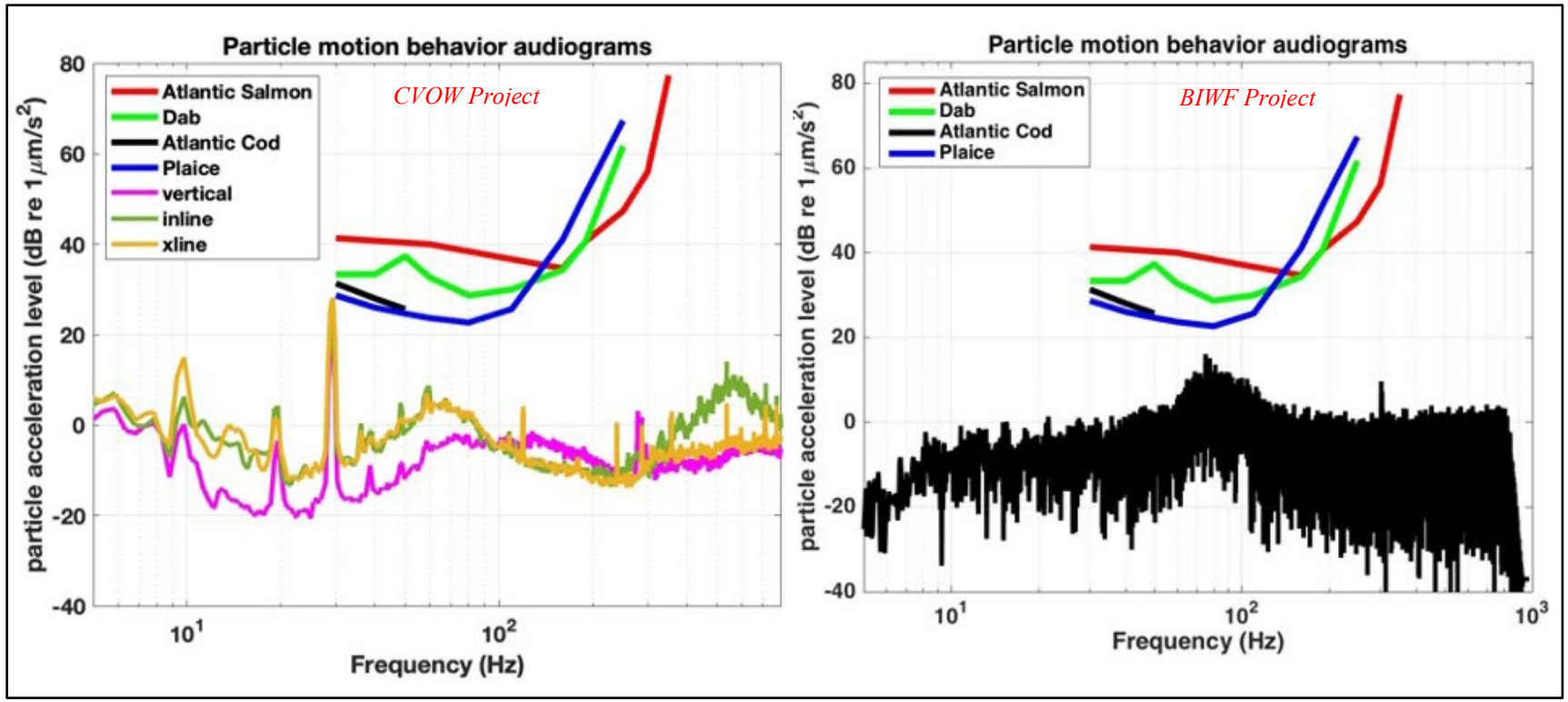

Figure 15. Particle acceleration level compared to behavioral audiograms of some fish (left panel). 12 January 2022 at 08:02:00 UTC

Note: The right panel shows the similar comparison for BIWF vertical acceleration data.

2.3.3 Tetrahedral Array Data Analysis

Acoustic particle accelerations were computed from the gradient of the acoustic pressures using the following equation:

$$-\nabla p = \rho \frac{\partial \vec{u}}{\partial t}$$

Where

p is the acoustic pressure,
u is the acoustic particle velocity, and
ρ is the density of the medium.

The pressure gradient, ∇p, was calculated using data provided by four hydrophones arranged at the vertices of a tetrahedral array. The particle velocity was estimated by numerical integration of the estimated acceleration. A second-order digital integrator with fractional delay was used to implement polynomial integration (i.e., Simpson's Rule) of the acceleration time series (Crocker and Fratantonio 2016).

The tetrahedral array measurements provide an estimate of the particle motion in the water column (at 1 m from the seabed), whereas the OBXs measured the particle velocity at the water-sediment interface. The OBX measures shear and interface waves (Scholte) in addition to compressional waves, whereas the water column measurements consist mostly of compressional waves. Interface waves (Scholte waves) have maximum amplitude at the water-sediment interface and decay exponentially with distance away (both in the sediment and water) from the seabed. Vibrations in the sediment are particularly important for benthic invertebrates (Roberts and Elliot 2017) in addition to fishes. The presence of Scholte waves can be explored using the OBX data (since these waves will be stronger in the OBX data compared to tetrahedral data) by investigating the three components of particle motion.

Figure 16 shows sample spectrograms (2-minute duration) from the hydrophones on the tetrahedral array (right panel) and the geophone channels (left panel). Few tonals are present in the hydrophone and geophone data.

Figure 17 shows an example of the particle velocity calculated using the hydrophone data for the same time period as in **Figure 10**.

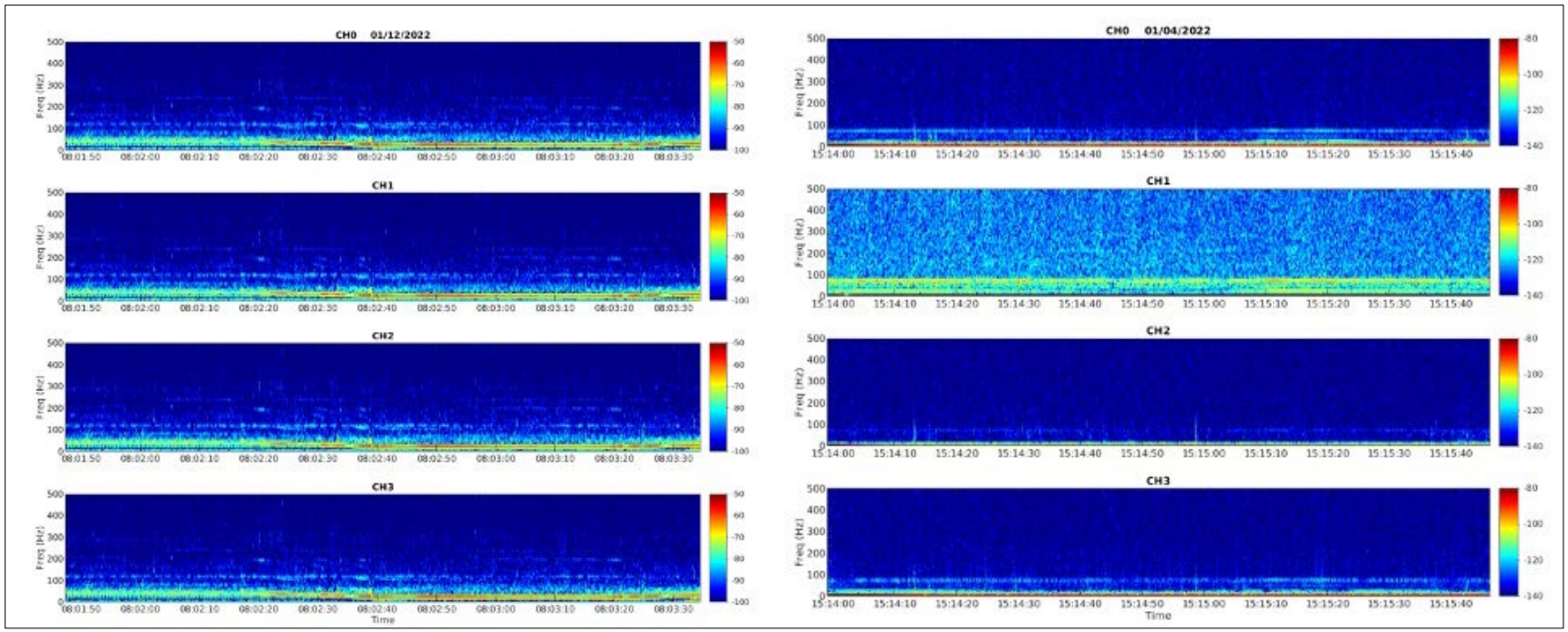

Figure 16. Spectrograms (2-minute duration) from the tetrahedral array (right panel) and the geophone channels (left panel)

Note: CH = Channel

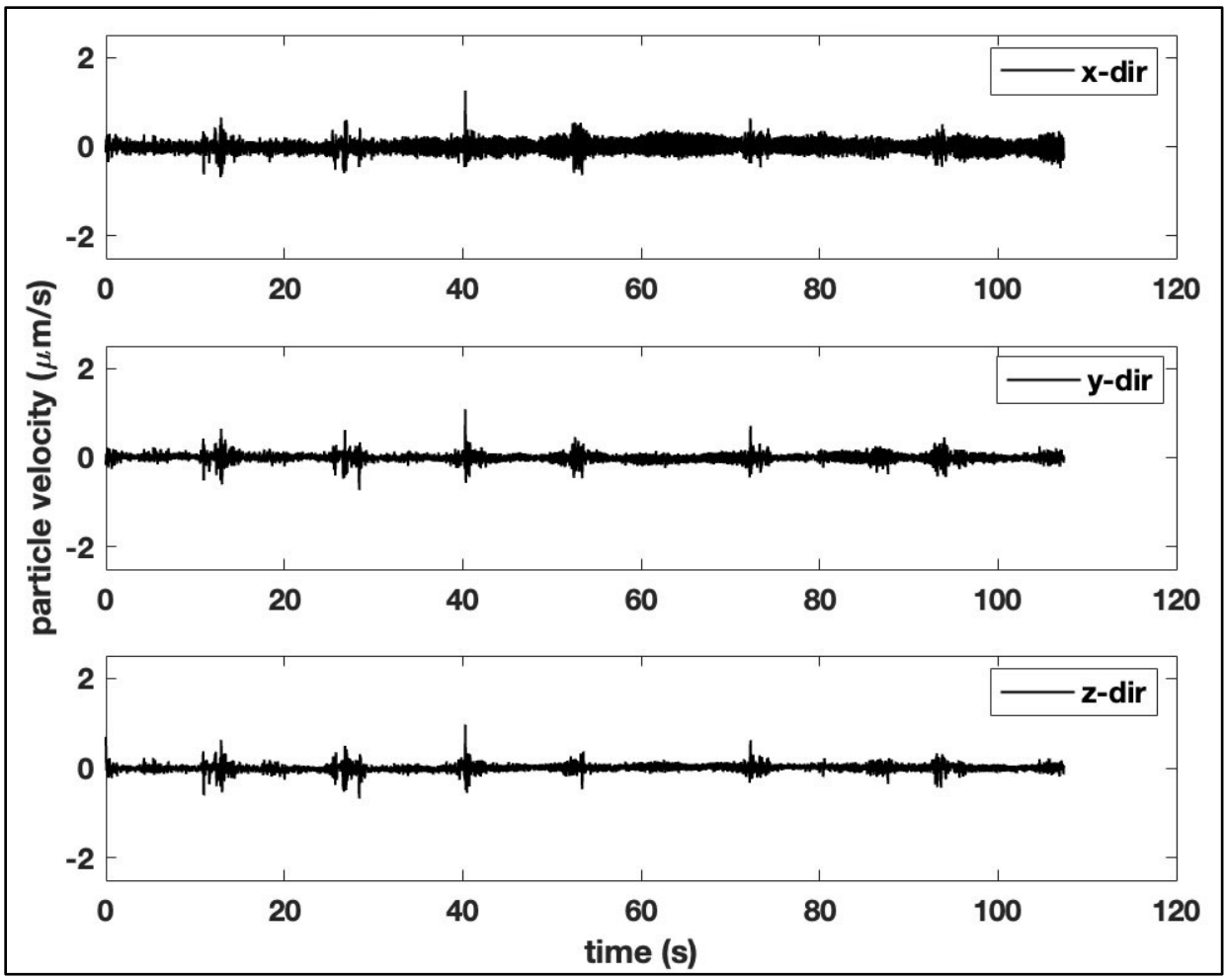

Figure 17. Particle velocity components calculated using the acoustic pressure measured on the tetrahedral array from 12 January 2022 at 08:02 UTC

Figure 18 shows the rms values of the velocity data shown in **Figure 17**. Therms values were calculated from the velocity and pressure data calculated for the tetrahedral array data for the time period of 12 January 2022, starting at 08:02:00 UTC. The rms values are calculated over 1-second time windows for the three particle velocity components (x, y, and z) and acoustic pressure.

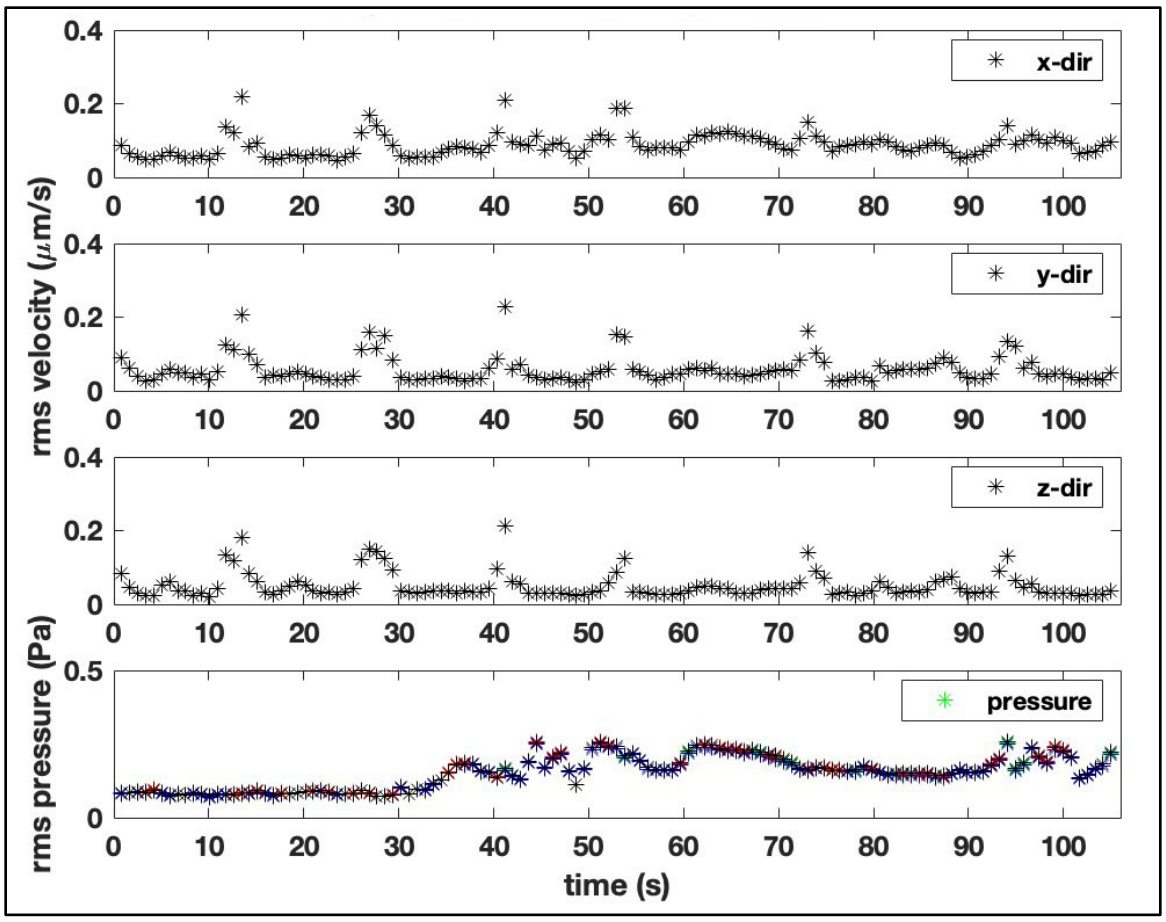

Figure 18. Rms values of the particle velocity and pressure for the data shown in Figure 17 starting at 08:02 UTC on 12 January 2022

Note: The rms values were calculated for a time window of 0.42 sec.

Figure 19 shows the power spectral density of the particle velocity data shown in **Figure 18**. **Figure 20** shows the acoustic pressure spectra calculated for the data shown on 12 January 2022 (08:02:00 UTC) for 0.42-second-long segments. The average of these segments is shown as the white curve. This figure also shows the power spectral density during operation from the BIWF data (red curve). Note that the BIWF data were measured at 50 m from the turbine, whereas CVOW data are measured at 350 m. The dashed red line in **Figure 20** shows the BIWF data extrapolated to 350 m by accounting for cylindrical spreading and absorption (0.025 dB per m).

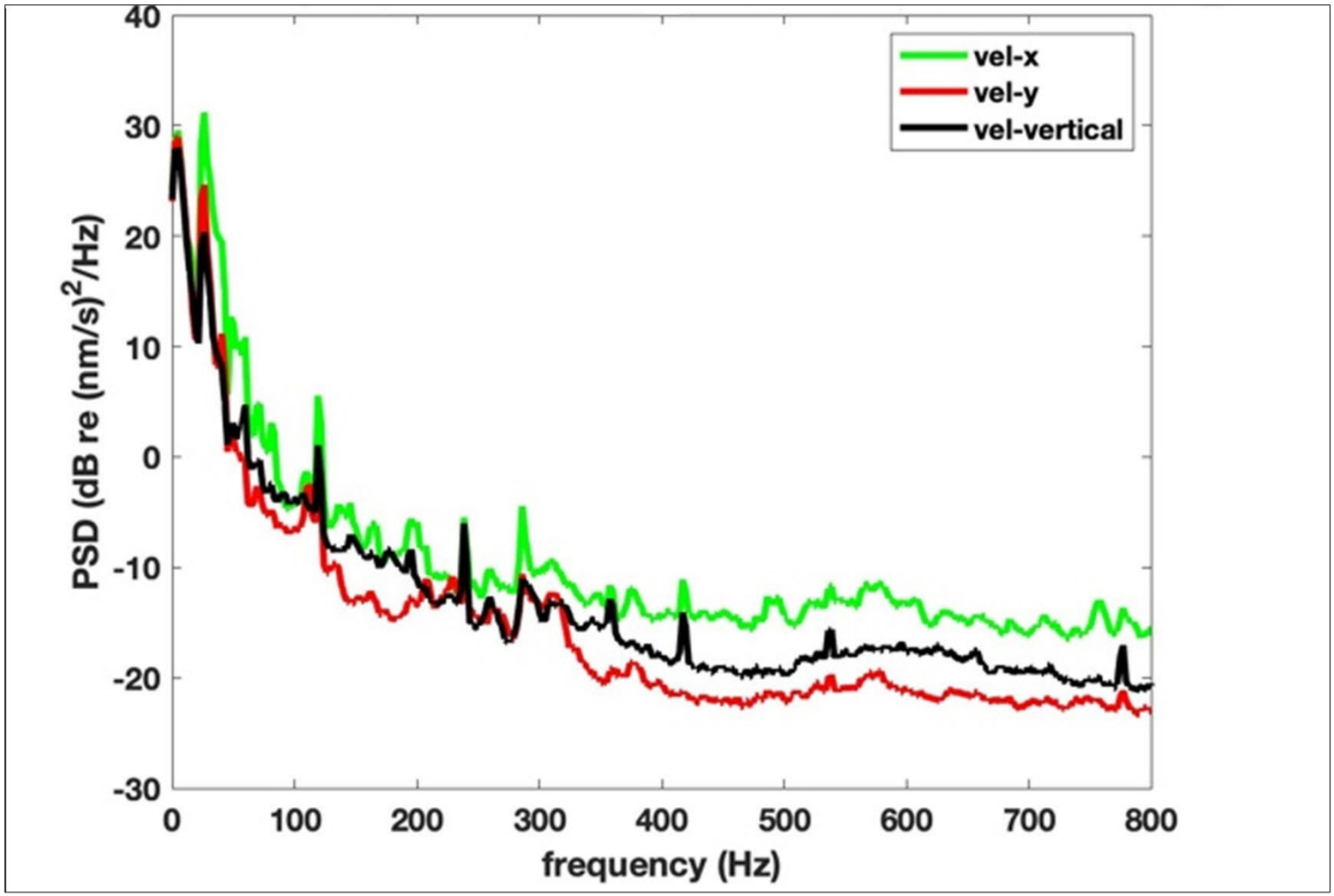

Figure 19. Spectra of the velocity data shown in Figure 17 (12 January 2022; 08:02:00 UTC)

Note: nm/s = nautical mile per second

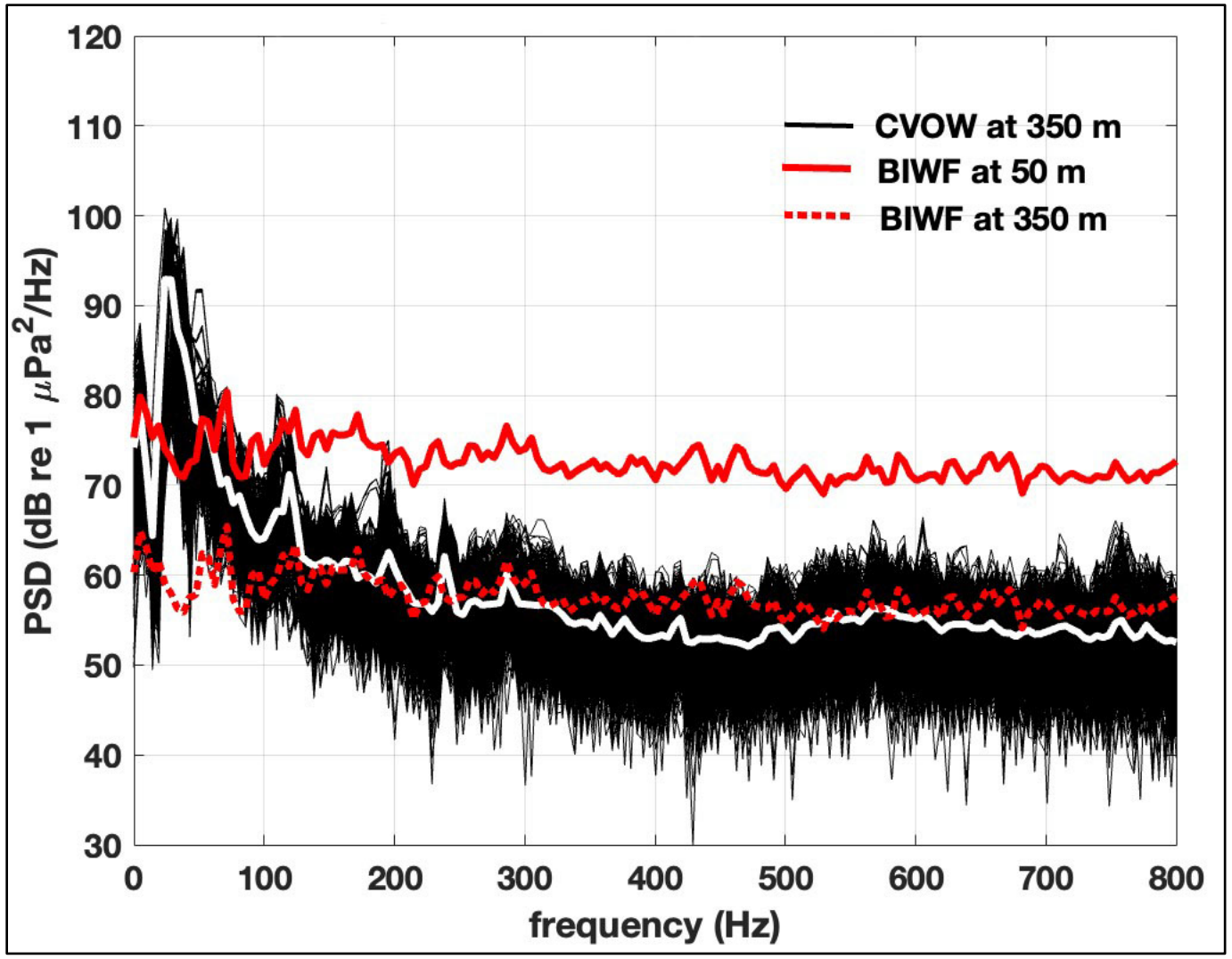

Figure 20. Comparison of power spectral density of acoustical pressure data from tetrahedral data from CVOW and BIWF

Note: The white and dashed red curves are the average values from CVOW and BIWF, respectively. The BIWF data (measured at 50 m) is adjusted for cylindrical spreading and absorption to extrapolate to 350 m. Spectra were calculated over 0.42-second-long intervals. The average spectra are shown as the white curve. Note that the time series for CVOW is plotted for a duration of 10 minutes and the spectrogram for BIWF is for a duration of 1 minute.

The noise data in **Figure 20** show that CVOW levels are substantially (10 to 30 dB) higher than BIWF levels in the frequency below approximately 120 Hz. It is hypothesized that the higher operational noise is due to vibrations in the CVOW monopile structure. The BIWF foundations are lattice-jacket structures with four legs, and no detectable structural vibration was measured. The CVOW foundations are monopiles, and it is probable that the structures are vibrating and transmitting this vibrational energy into the water column and seabed. This subject needs more study, both for the structural vibration mechanisms and the potential biological effects.

Figure 21 shows the particle acceleration spectral level calculated from the pressure data from the tetrahedral array (data correspond to 12 January 2022, 08:02:00 UTC). The particle acceleration is expressed in dB referenced to 1 $\mu m/s^2$ so it can be compared to published behavioral audiograms of fish (e.g., Atlantic salmon, dab, Atlantic cod, plaice). These hearing sensitivity curves can be compared to the particle acceleration levels for the x, y, and z components. It can be seen that the particle acceleration levels are below the hearing threshold of all fish considered here. This finding is consistent with observations made during similar operational phase monitoring conducted for the BIWF Project (HDR 2019).

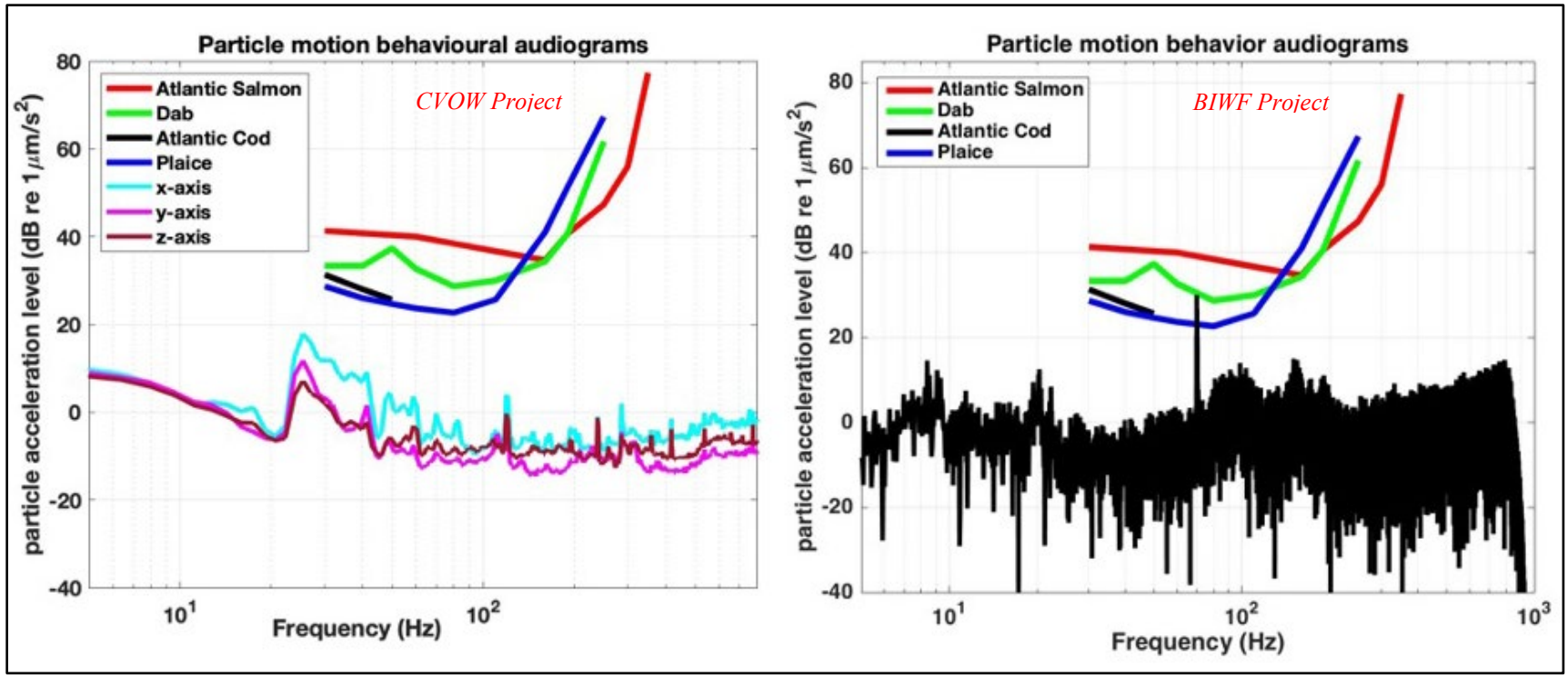

Figure 21. Particle acceleration levels compared with behavioral audiograms of four fish species

Note: These data are from the tetrahedral array showing the acceleration levels at 1 m above the seafloor. The right panel shows the similar comparison for BIWF vertical acceleration data.

2.4 Conclusion, Discussion, and Recommendations for Future Monitoring

Data analysis indicated that underwater sound levels recorded (approximately 350 m from Turbine A02) during turbine operations at CVOW were relatively low (the received levels ranged between 120 and 130 dB re 1 µPa, except during storms when the received levels increased to 145 dB re 1 µPa). Recorded particle acceleration levels were also low. These were compared to published behavioral audiograms of selected fish (e.g., Atlantic salmon, dab, Atlantic cod, plaice) and found to be below the hearing threshold of these fish. Overall, all recorded measurements were below the temporary threshold shift (TTS) and permanent threshold shift (PTS) onset criteria recommended by the National Marine Fisheries Service (NMFS) Marine Mammal Guidance[4] (NMFS 2018).

Operational phase sound levels recorded at CVOW were measurably higher than those previously recorded at the BIWF at frequencies below approximately 120 Hz. It is hypothesized that the higher operational noise recorded at CVOW is due to vibrations in the monopile structures. The BIWF foundations are lattice-jacket structures with four legs and have no detectable structural vibrations. It is possible that CVOW monopile foundations vibrate when the turbines are operating, and the vibrational energy is transmitted into the water column and seabed. This hypothesis needs additional investigation, both for the structural vibration mechanisms and potential biological effects.

At frequencies above 120 Hz, CVOW's operational phase monitoring results are broadly consistent with operational phase acoustic monitoring previously conducted at wind farms in the U.S. (BIWF) and Europe. At the BIWF, for example, underwater sound levels recorded at 50 m from operational turbines were near background (ambient) levels, and often not measurable due to other natural and anthropogenic noise (waves or boat sounds) (HDR 2019). There are, however, some important caveats to note when making such a comparison, including the differences in size and structure of European turbines versus those used at BIWF and CVOW. Additionally, CVOW and BIWF results are not directly comparable due to differences in foundation type and other key variables. Recorded operational sound levels at the BIWF (approximately 100 dB re 1µPa rms measured at a distance of 50 m at a frequency of 70 Hz) were below the TTS and PTS onset criteria recommended by the NMFS Marine Mammal Guidance (NMFS 2018).

Similar studies conducted in Europe indicate that operational noise from wind farms is continuous in nature and is characterized by tonal components at frequencies below 1,000 Hz (Degn 2000; Betke et al. 2004; Madsen et al. 2006; Wahlberg and Westerberg 2005; Tougaard et al. 2009; Sigray and Andersson 2011). Although operational wind farms produce broadband low-frequency noise, operational noise tends to be of low amplitude and is relatively localized (Madsen et al. 2006; Evans 2008; Wilhelmsson et al. 2010; Scheidat et al. 2011; Mooney et al. 2020). As a result, the risk of negative impacts to protected marine species such as marine mammals are expected to be minor, as low noise levels make injury or masking highly unlikely (Madsen et al. 2006; Bailey et al. 2014; Verfuss et al. 2015; Tougaard 2018).

2.4.1 Recommendations for Future Monitoring

Because of the low sound levels recorded during operational monitoring conducted under the RODEO Program at CVOW and BIWF, and the very low probability of these sounds causing potential harm to fish and marine mammals, operational phase underwater acoustic monitoring may not provide significant additional value for future facilities. As part of a risk mitigation plan, this monitoring may be curtailed. Note that to date, operational noise and particle motion monitoring for offshore wind farms in the U.S.

[4] The behavioral harassment threshold for non-impulsive sound is 120 dB, and the TTS and PTS thresholds mentioned are above 150 dB (metric is the weighted cumulative sound exposure level).

has only been conducted adjacent to relatively smaller wind farms (five turbines at the BIWF and two turbines at CVOW). It is possible that when the number of turbines present is significantly higher (hundreds of turbines arranged in a complex geometrical pattern), the cumulative impact from operational sounds could be different than what has been reported for smaller facilities. It is therefore recommended that operational phase sound monitoring be conducted for at least one or two larger future planned facilities to determine the combined effects of many simultaneously operating turbines and any possible azimuthal variation due to wind farm geometry.

The issue of monopile foundations versus lattice-jacket foundations should also be investigated further. One possible approach is to model the two foundations using finite element methods and confirm the higher noise radiated from the monopiles.

2.4.2 Recommendations for Additional Data Analysis

In addition to the analysis and results reported in this volume, data collected during the operational phase may be used in the future for conducting additional data analysis, such as:

1. Identifying:
    a. ambient noise spectrum and determining how it changed over time,
    b. when and what portions of the operational noise is in the ambient noise, and
    c. harmonics in particle motion and pressure data;
2. Quantifying the spectrum and levels of operational noise as a function of wind speed and rpm;
3. Comparing particle motion and pressure;
4. Assessing how the operational noise can be demodulated and analyzed; and
5. Evaluating how some of the oscillatory components of supporting data (e.g., water depth and others) can be identified and quantified.

3 References

Bailey H, Brookes K, Thompson P. 2014. Assessing environmental impacts of offshore wind farms: lessons learned and recommendations for the future. Aquat Biosyst. 10(1):article 8. https://doi.org/10.1186/2046-9063-10-8.

Betke K, Glahn S, Matuschek R. 2004. Underwater noise emissions from offshore wind turbines. In: Cassereau D, editor. Proceedings of CFA/DAGA'04; March 22–25, 2004; Strasbourg, France. Paris (FR): Société Française d'Acoustique. p. 591–592. http://www.conforg.fr/cfadaga2004/master_cd/cd1/articles/000516.pdf.

Crocker SE, Fratantonio FD (Naval Undersea Warfare Center Division, Newport, RI). 2016. Characteristics of sounds emitted during high-resolution marine geophysical surveys. Herndon (VA): Bureau of Ocean Energy Management. Naval Undersea Warfare Center Division New Port (NUWC-NPT) Technical Report 12,203 and OCS Study BOEM 2016-044.

Degn U. 2000. Offshore wind turbines – VVM: underwater noise measurements, analysis, and predictions. Haslev (DK): Odegaard & Danneskiold-Samsoe A/S. Report No. 00-792.

Evans P. 2008. Offshore wind farms and marine mammals: impacts & methodologies for assessing impacts. Bangor (GB): University of Bangor.

HDR. 2019. Field observations during wind turbine operations at the Block Island Wind Farm, Rhode Island. Final Report to the U.S. Department of the Interior, Bureau of Ocean Energy Management, Office of Renewable Energy Programs. Report No. OCS Study BOEM 2019-028.

HDR. 2020. Field Observations During Offshore Wind Structure Installation and Operation, Volume I. Final Report to the U.S. Department of the Interior, Bureau of Ocean Energy Management, Office of Renewable Energy Programs. Contract No. M15PC00002. Report No. OCS Study BOEM 2021-225. 332 pp.

Hobiger M, Bard PY, Cornou C, Le Bihan N. 2009. Single station determination of Rayleigh wave ellipticity by using the random decrement technique (RayDec). Geophys Res Lett. 36(14): L14303.

Lindell H. 2003. Utgrunden off-shore wind farm: measurements of underwater noise. Göteborg (SE): Ingemansson Technology AB. Report 11–00329-03012700-eng.

Madsen PT, Wahlberg M, Tougaard J, Lucke K, Tyack P. 2006. Wind turbine underwater noise and marine mammals: implications of current knowledge and data needs. Mar Ecol Prog Ser. 309:279–295.

Marmo B, Roberts I, Buckingham MP, King S, Booth C. 2013. Modelling of noise effects of operational offshore wind turbines including noise transmission through various foundation types. Edinburgh (GB): Scottish Government.

Mooney TA, Andersson MH, Stanley J. 2020. Acoustic impacts of offshore wind energy on fishery resources: An evolving source and varied effects across a wind farm's lifetime. Oceanography 33(4):82–95. https://doi.org/10.5670/oceanog.2020.408.

National Marine Fisheries Service. 2018. 2018 Revision to technical guidance for assessing the effects of anthropogenic sound on marine mammal hearing (Version 2.0): underwater thresholds for onset of

permanent and temporary threshold shifts. Silver Spring (MD): U.S. Dept. of Commerce, NOAA Fisheries. NOAA Technical Memorandum NMFS-OPR-59.

Roberts L, Elliott M. 2017. Good or bad vibrations? Impacts of anthropogenic vibration on the marine epibenthos. Sci Total Environ. 595:255–268.

Scheidat M, Tougaard T, Brasseur S, Carstensen J, van Polanen Petel T, Teilmann J, Reijnders P. 2011. Harbour porpoises (*Phocoena phocoena*) and wind farms: a case study in the Dutch North Sea. Environ Res Lett. 6(2):025102.

Sigray P, Andersson MH. 2011. Particle motion measured at an operational wind turbine in relation to hearing sensitivity in fish. J Acoust Soc Am. 130:200–207. https://doi.org/10.1121/1.3596464.

Tougaard J. 2018. Pile driving and porpoises, Tyra pipeline valve stations. Copenhagen (DK): Maersk Oil og Gas.

Tougaard J, Henriksen OD, Miller LA. 2009. Underwater noise form three types of offshore wind turbines: Estimation of impact zones for harbor porpoises and harbor seals. J Acoust Soc Am. 125:3766–3773.

Tougaard J, Hermannsen L, Madsen PT. 2020. How loud is the underwater noise from operating offshore wind turbines? J Acoust Soc Am. 148:2885. https://doi.org/10.1121/10.0002453.

Verfuss U, Sparling C, Arnot C, Judd A, Coyle M. 2015. Review of offshore wind farm impact monitoring and mitigation with regard to marine mammals. Adv Exp Med Biol. 875:1175–1182. https://doi.org/10.1007/978-1-4939-2981-8_147.

Wahlberg M, Westerberg H. 2005. Hearing in fish and their reactions to sounds from offshore wind farms. Mar Ecol Prog Ser. 288:295–309.

Wilhelmsson D, Malm T, Thompson R, Tchou J, Sarantakos G, McCormick N, Luitjens S, Gullström M, Patterson Edwards JK, Amir O, Dubi A (eds). 2010. Greening blue energy: identifying and managing the biodiversity risks and opportunities of offshore renewable energy. Gland (CH): IUCN (International Union for Conservation of Nature).

Appendix A: Hydrophone and Geophone Sensitivity Curves

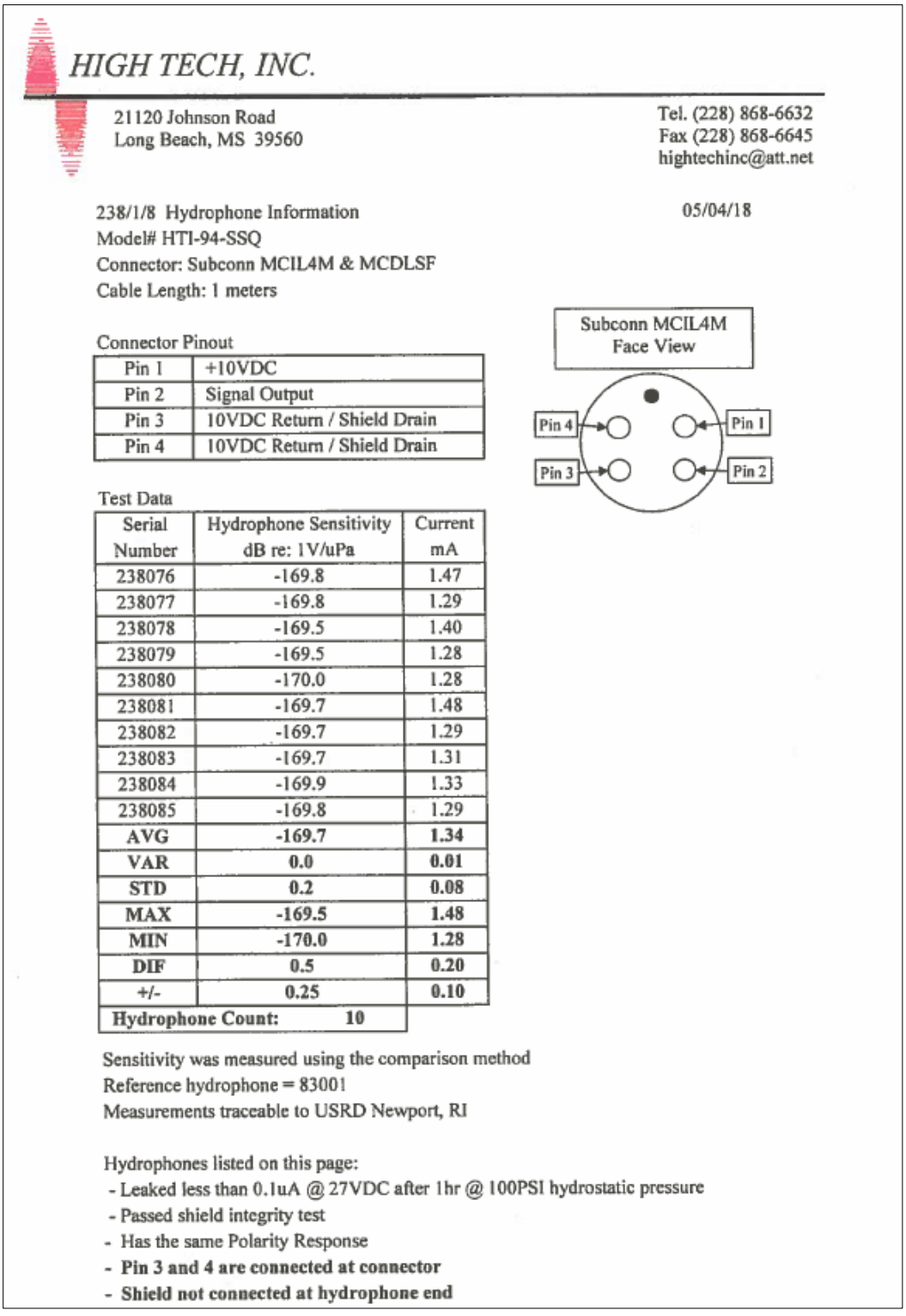

HIGH TECH, INC.

21120 Johnson Road
Long Beach, MS 39560

Tel. (228) 868-6632
Fax (228) 868-6645
hightechinc@att.net

238/1/8 Hydrophone Information 05/04/18
Model# HTI-94-SSQ
Connector: Subconn MCIL4M & MCDLSF
Cable Length: 1 meters

Connector Pinout

Pin 1	+10VDC
Pin 2	Signal Output
Pin 3	10VDC Return / Shield Drain
Pin 4	10VDC Return / Shield Drain

Test Data

Serial Number	Hydrophone Sensitivity dB re: 1V/uPa	Current mA
238076	-169.8	1.47
238077	-169.8	1.29
238078	-169.5	1.40
238079	-169.5	1.28
238080	-170.0	1.28
238081	-169.7	1.48
238082	-169.7	1.29
238083	-169.7	1.31
238084	-169.9	1.33
238085	-169.8	1.29
AVG	**-169.7**	**1.34**
VAR	**0.0**	**0.01**
STD	**0.2**	**0.08**
MAX	**-169.5**	**1.48**
MIN	**-170.0**	**1.28**
DIF	**0.5**	**0.20**
+/-	**0.25**	**0.10**
Hydrophone Count:	**10**	

Sensitivity was measured using the comparison method
Reference hydrophone = 83001
Measurements traceable to USRD Newport, RI

Hydrophones listed on this page:
- Leaked less than 0.1uA @ 27VDC after 1hr @ 100PSI hydrostatic pressure
- Passed shield integrity test
- Has the same Polarity Response
- **Pin 3 and 4 are connected at connector**
- **Shield not connected at hydrophone end**

Geosled hydrophone sensitivity

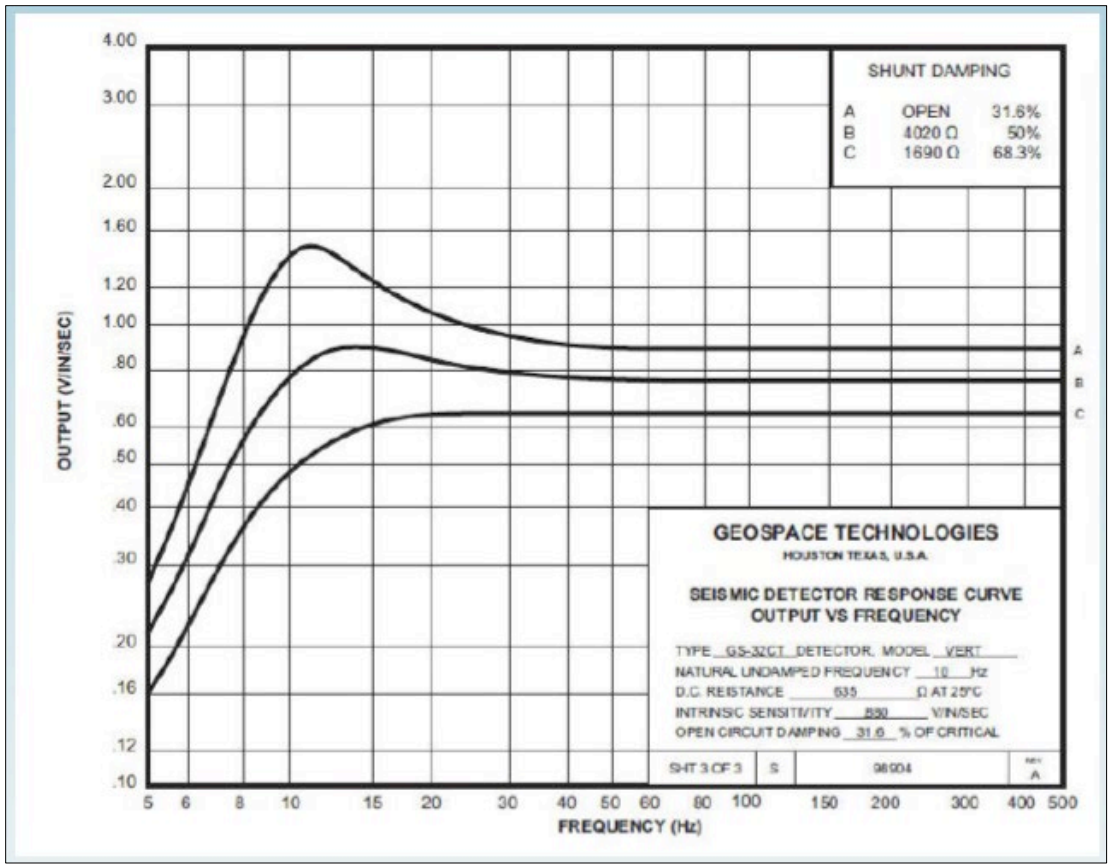

Geophone sensitivity

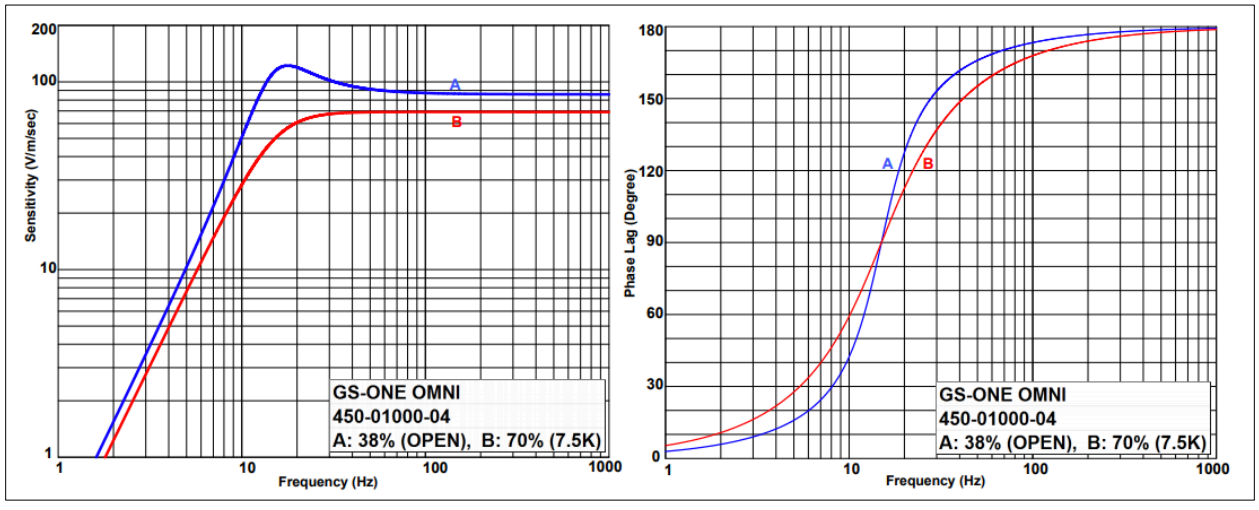

Ocean Bottom Recorders Geophone and Hydrophone Sensor System (OBX) 15-hertz GS-One Geophone on each axis

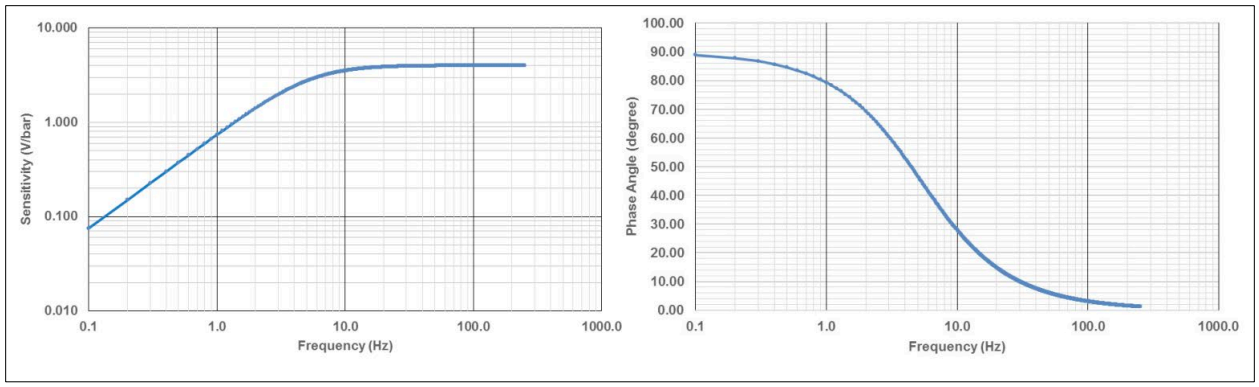

OBX Deepender Hydrophone

Notes: Converting 4 V/bar to dB re volt per micropascal (V/µPa).
1 bar is 10^{11} µPa so max sensitivity is $4x10^{-11}$ V/µPa or -208 dB re V/µPa.

U.S. Department of the Interior (DOI)
DOI protects and manages the Nation's natural resources and cultural heritage; provides scientific and other information about those resources; and honors the Nation's trust responsibilities or special commitments to American Indians, Alaska Natives, and affiliated island communities.

Bureau of Ocean Energy Management (BOEM)
BOEM's mission is to manage development of U.S. Outer Continental Shelf energy and mineral resources in an environmentally and economically responsible way.

BOEM Environmental Studies Program
The mission of the Environmental Studies Program is to provide the information needed to predict, assess, and manage impacts from offshore energy and marine mineral exploration, development, and production activities on human, marine, and coastal environments. The proposal, selection, research, review, collaboration, production, and dissemination of each of BOEM's Environmental Studies follows the DOI Code of Scientific and Scholarly Conduct, in support of a culture of scientific and professional integrity, as set out in the DOI Departmental Manual (305 DM 3).